5-29-1961

Adaptation of Beggs Deformeter Apparatus to the Solution of Three-Dimensional Problems

Roland L. Finley

ADAPTATION OF BEGGS DEFORMETER APPARATUS TO THE SOLUTION OF THREE-DIMENSIONAL PROBLEMS

By

Roland L. Finley

A Thesis

Submitted in Partial Fulfillment of the

Requirements for the Degree of

Master of Science in Engineering

The University of New Mexico

1961

ADAPTATION OF FINITE DIFFERENCE METHODS TO THE SOLUTION OF THREE-DIMENSIONAL PROBLEMS

by

Roland L. Finley

A Thesis

Submitted in Partial Fulfillment of the

Requirements for the Degree of

Master of Science in Engineering

The University of New Mexico

1961

This thesis, directed and approved by the candidate's committee, has been accepted by the Graduate Committee of the University of New Mexico in partial fulfillment of the requirements for the degree of

MASTER OF SCIENCE

C. A. Castetter
Dean

May 29, 1961
Date

Thesis committee

Eugene Zwoyer
Chairman

M. M. Cottrell

Lay Foss

ACKNOWLEDGMENT

The author is most appreciative of the time, interest, guidance and advise received during the preparation of this thesis from Doctor Eugene M. Zwoyer who acted as chairman of the thesis committee.

Appreciation is also extended to Professors Raymond J. Foss and Marion M. Cottrell for helpful comments and suggestions, during the making of this study.

The author is indebted to Dwight F. Denton for much information concerning the use of the Beggs deformeter equipment and for permission to use Figures 2, 3, 4, 5, and 6 of this thesis which were reproduced from "An Evaluation of the Beggs Deformeter".

A special thanks is extended to the authors wife, Fay, for encouragements and moral support which was essential in the making of this report.

Roland L. Finley

Albuquerque, New Mexico

April, 1961

ACKNOWLEDGMENT

The author is most appreciative of the kind interest, guidance and advice received during the preparation of this thesis from Doctor Eugene M. Sawyer who acted as chairman of the thesis committee.

Appreciation is also extended to Professors Maynard J. Foss and Marion M. Cottrell for helpful comments and suggestions, during the making of this study.

The author is indebted to Dwight F. Benton for much information concerning the use of the Begge deformeter equipment and for permission to use Figures 2, 3, 4, 5, and 6 of this thesis which were reproduced from "An Investigation of the Begge Deformeter".

A special thanks is extended to the authors wife, Fay, for encouragements and moral support which was essential in the making of this report.

Roland D. Finley

Albuquerque, New Mexico

April, 1961

CONTENTS

CONTENTS

CHAPTER

LIST OF FIGURES

LIST OF FIGURES

FIGURES

LIST OF TABLES

LIST OF TABLES

TABLE PAGE

TABLE

TABLE

CHAPTER I

INTRODUCTION

In the area of structural analysis and structural design, numerous efforts have been made and more are yet to be made toward solving statically indeterminate problems easily and with a high degree of accuracy. Fortunately, the great majority of such problems can be solved by one or more of the many mathematical methods that are normally used. However, the mathematical solutions become exceedingly difficult if and when it is desired to use irregularly shaped structural members.

Simplifying assumptions are used extensively in structural analysis to transform complicated three-dimensional problems into less complicated two-dimensional problems. While most of these assumptions are based on experience and are usually of such a nature as to ensure the safety of the structure, the effect that a structural member in the third dimension may have upon a coplanar frame is not always easily interpreted by the analyst. Consequently, this condition can and often does establish an unsafe link in an otherwise completely well designed

CHAPTER I

INTRODUCTION

structure. On the other hand, in areas of analytic uncertainties, the designer often uses more material than is needed to offset possible failures.

Many structures that are to be designed and used in the present air and space age will not tolerate the use of such simplifying assumptions and excessive quantities of materials to ensure structural safety. In order to meet present demands, many design organizations rely on trial and error solutions based first on a rough mathematical design for a proto type then secondly on the results obtained from testing the proto type for both over design and under design. For many structures, this type of design is economically feasible and, in general, produces efficient usage of materials. Certain other structures are such that trial and error solutions of the kind just mentioned are not applicable. For most custom built structures such as bridges, buildings, dams, and towers; proto types are too expensive, and for many of these, rigorous mathematical solutions for design are practically impossible. To augment this dilemma, several mechanical

structure. On the other hand, in spite of analytic uncertainties, the designer often uses more material than is needed to effect possible failures.

Many structures that are to be designed and used in the present air and space age will not tolerate the use of such simplifying assumption and excessive quantities of materials to ensure structural safety. In order to meet present demands, many design organizations rely on trial and error solutions based first on a rough mathematical design for a proto type then secondly on the results obtained from testing the proto type for both over design and under design. For many structures, this type of design is economically feasible and, in general, produces efficient usage of materials. Certain other structures are such that trial and error solutions of the kind just mentioned are not applicable. For most custom built structures such as bridges, buildings, dams, and towers; proto types are too expensive, and for many of these, rigorous mathematical solutions for design and practically impossible. To augment this dilemma, several restrictive

methods have been devised to assist in the solutions of structural problems [1, 2, 3, and 4]; but unfortunately, most of the available methods are only applicable to solutions of coplanar problems. In some cases, the third dimension can possibly be included; but, as of yet little effort has been put forth in this direction. Consequently, practically no information in this field is available to the design engineer.

The Beggs method [5, 6, and 7] is a method devised for determining experimentally, bending moments, shears, and axial forces in structural members. Of the many methods available, the Beggs method is probably the most widely used and has possibilities of being extended to include solutions of three-dimensional problems. [8] For this reason and the fact that the necessary equipment was available, the author chose the Beggs method to investigate some three-dimensional problems for purposes of making recommendations for possible design changes to

---

Superscript numerals correspond to bibliographical entries.

methods have been devised to assist in the solution of structural problems [1, 2, 3, and 4], but unfortunately, most of the available methods are only applicable to solutions of coplanar problems. In these cases, the third dimension can possibly be included, but as of yet little effort has been put forth in this direction. Consequently, practically no information in this field is available to the design engineer.

The Beggs method [5, 6, and 7] is a method devised for determining experimentally, bending moments, shears, and axial forces in structural members. Of the many methods available, the Beggs method is probably the most widely used and has possibilities of being extended to include solutions of three-dimensional problems. For this reason and the fact that the necessary equipment was available, the author chose the Beggs method to investigate some three-dimensional problems, for purposes of making recommendations for possible design changes to

---

Superscript numerals correspond to bibliographical entries.

the present apparatus found desirable in measuring and inducing deflections.

The Beggs deformeter apparatus was designed to be used in the solution of coplanar problems only; however, it is conceivable that the design could be altered to include solutions to problems involving the third dimension. In order to determine what changes were necessary, or at least desirable, two three-dimensional problems were selected for solution in this thesis. Both problems selected are very common to the structural designer; however, the design of such structures is usually based on crude, overly simplified mathematical analysis.

Detailed discussions of each problem are presented in later chapters which point out the necessary improvisions required in the solutions of three-dimensional problems with the present apparatus. Several "pitfalls" are pointed out along with ways of avoiding them. A short discussion concerning theoretical principles used in conjunction with the experimental procedures is presented early in this report to familiarize the reader with the ideas being pursued.

the present apparatus found desirable in measuring two inducing deflections.

The Beggs deformeter apparatus was designed to be used in the solution of coplanar problems only. However, it is conceivable that the design could be altered to include solutions to problems involving the third dimension. In order to determine what changes were necessary, or at least desirable, two three-dimensional problems were selected for solution in this thesis. Both problems selected are very common to the structural designer; however, the design of such structures is usually based on crude, overly simplified mathematical analysis.

Detailed discussions of each problem are presented in later chapters which point out the necessary improvements required in the solutions of three-dimensional problems with the present apparatus. Several "pitfalls" are pointed out along with ways of avoiding them. A short discussion concerning theoretical principles used in conjunction with the experimental procedures is presented early in this report to familiarize the reader with the ideas being pursued.

Proposals for redesign of the present equipment found desirable during the investigations of the example problems are presented along with appropriate drawings. For obvious reasons, no attempt was made to present rigorous mathematical solutions to the example problems. Only simplified mathematical checks are presented for comparison purposes.

Proposals for redesign of the present department towns
desirable during the investigations of the managed problems
are presented along with appropriate drawings. For obvious
reasons, no attempt was made to present complete mathematical
solutions to the example problems. Only simplified mathe-
matical checks are presented for comparison purposes.

CHAPTER II

THEORETICAL PRINCIPLES

The Beggs deformeter apparatus was originally designed to aid in the determination of influence lines for coplanar structures. For this, Müller-Breslau's principle for obtaining influence lines is used. This principle may be stated as follows:

> The ordinates of the influence line for any stress element (such as axial stress, shear, moment, or reaction) of any structure are proportional to those of the deflection curve which is obtained by removing the restraint corresponding to that element from the structure and introducing in its place a deformation into the primary structure which remains. [9]

An adaptation of this principle per se to include a third dimension would necessitate the determination of an influence surface in place of an influence line. Since non-coplanar surfaces are difficult to illustrate, the above principle was used only to determine certain desired stress elements caused by unit loads being applied at preselected load points. The stress elements determined in the solutions of the example problems presented in this thesis consists only of reactions located at fixed supports;

CHAPTER II

THEORETICAL PRINCIPLES

The Beggs deformeter apparatus was originally designed to aid in the determination of influence lines for complex structures. For this, Müller-Breslau's principle for constructing influence lines is used. This principle may be stated as follows:

> The ordinates of the influence line for any stress element (such as axial stress, shear, moment, or reaction) of any structure are proportional to those of the deflection curve which is obtained by removing the restraint corresponding to that element from the structure and introducing in its place a deformation into the primary structure which remains. [2]

An adaptation of this principle per se to influence lines of a third dimension would necessitate the determination of an influence surface in place of an influence line. Since non-coplanar surfaces are difficult to illustrate, the above principle was used only to determine certain desired stress elements caused by unit loads being applied at preselected load points. The stress elements determined in the solutions of the example problems presented in this thesis consists only of reactions located at fixed supports

however, one should not lose sight of the possibility of determining stress elements located elsewhere in the structure.

After solving for reactions caused by the above mentioned unit loads, the principle of super position was used to transform these reactions into magnitudes corresponding to actual loading conditions. The combination of the principle of super position with Müller-Breslau's principle as heretofore described results in the fulfillment of Betti's law which may be stated as follows:

> In any structure the material of which is elastic and follows Hooke's law and in which the supports are unyielding and the temperature constant, the external virtual work done by system of forces P_m during the distortion caused by a system of forces P_n is equal to the external virtual work done by the P_n system during the distortion caused by the P_m system. [10]

An illustration of the two force systems is shown in Figure 1. Each force system is shown on a separate view of the structure for clarity only. It must be realized, of course, that the two systems necessarily act simultaneously on the same structure to satisfy Betti's law. This law may be stated in equation form as

however, one should not lose sight of the possibility of determining stress elements located elsewhere in the structure.

After solving for reactions caused by the above mentioned unit loads, the principle of super position was used to transform these reactions into equivalents corresponding to actual loading conditions. The combination of the principle of super position with Müller-Breslau's principle as heretofore described results in the Virtual-ment of Betti's law which may be stated as follows:

> In any structure the material of which is elastic and follows Hooke's law and in which the supports are unyielding and the temperature constant, the external virtual work done by system of forces P^m during the distortion caused by a system of forces P^v is equal to the external virtual work done by the P^v system during the distortion caused by the P^m system. [10]

An illustration of the two force systems is shown in Figure 1. Each force system is shown on a separate view of the structure for clarity only. It must be realized, of course, that the two systems necessarily act simultaneously on the same structure to satisfy Betti's Law. This law may be stated in equation form as

$$P_m \quad \Delta_{mn} = P_n \quad \Delta_{nm} \qquad (1)$$

where Δ_{mn} is the deflection of the point of application of one of the forces P_m (in the direction and sense of this force) caused by the application of the P_n force system and Δ_{nm} is the deflection of the point of application of one of the forces P_n caused by the application of the P_m force system.

For further explanation and verification of the principles and laws described in this chapter, reference is made to any of several good texts on statically indeterminate structures.

$$P_m \triangle_{ma} = P_n \triangle_{na} \qquad (7)$$

where $\triangle_{ma}$ is the deflection at the point of application of one of the forces P_m (in the direction and sense of this force) caused by the application of the P_n force system and $\triangle_{na}$ is the deflection of the point of application of one of the forces P_n caused by the application of the P_m force system.

For further explanation and verification of the principles and laws described in this chapter, reference is made to any of several good texts on structural indeterminate structures.

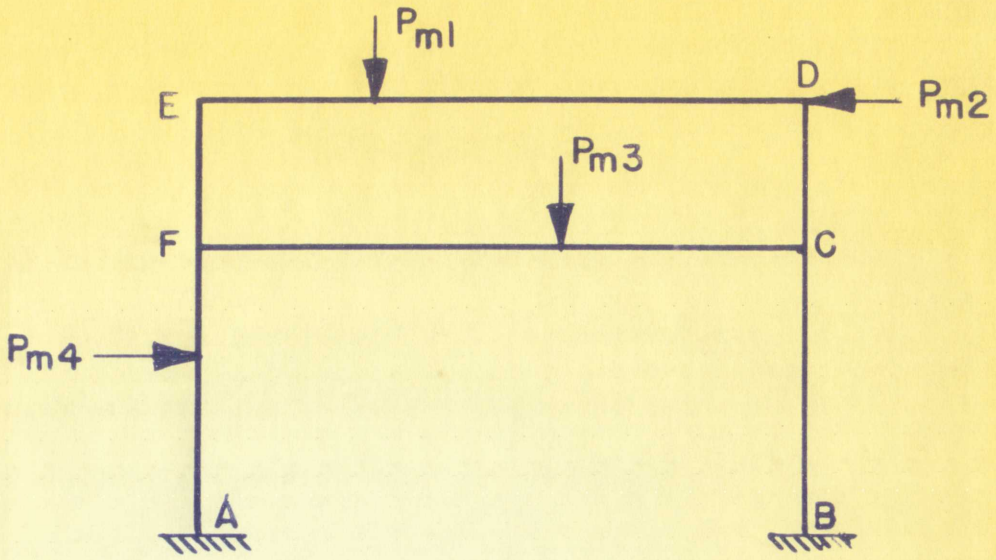

(a) P_m System

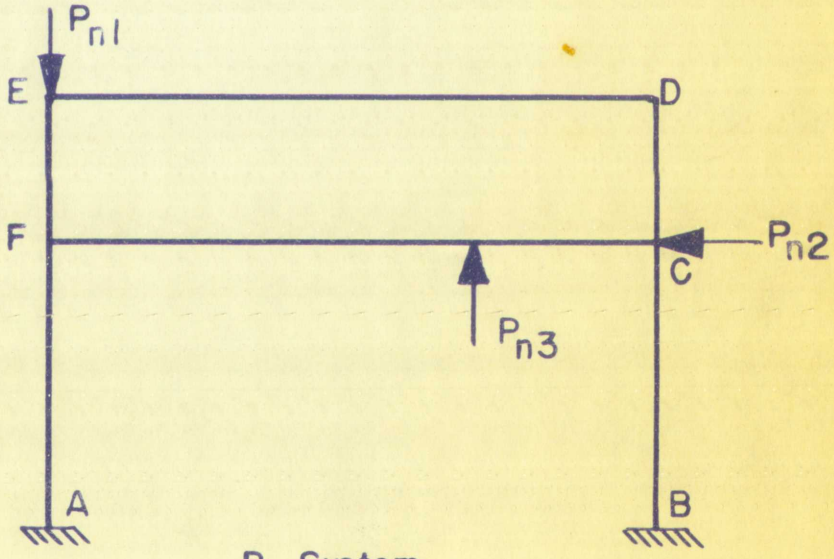

(b) P_n System

FIGURE 1

FORCE SYSTEMS

CHAPTER III

APPARATUS USED

A brief discussion is presented in this chapter which should give the reader enough information concerning various components used in setting up and solving problems by the Beggs method to permit the understanding of the chapters to follow. There is no attempt here or any where else in this thesis to explain in detail the functioning and calibration of the equipment to an extent necessary for the solution of problems. Reference is made to entries eleven and twelve of the bibliography for excellent detailed discussions on this subject.

Items of equipment that make up the Beggs deformeter apparatus are shown in Figure 2. Essential parts of this equipment includes two filar micrometer microscopes used to measure deflections at load points, six precision made gage clamps used to simulate reactions, and various sets of close tolerance distortion plugs used to induce angular and translation deflections at the reactions and at floating gage points.

CHAPTER III

APPARATUS USED

A brief discussion is presented in this chapter that should give the reader some information concerning strain components used in testing by and solving problems by the Beggs method to permit the understanding of the chapters to follow. There is no attempt here of any more than in that thesis to explain in detail the functioning and calibration of the equipment, to an extent necessary for the solution of problems. Reference is made to various standard works of the bibliography for sufficient explanations on this subject.

Items of equipment that take up the Beggs deformeter apparatus are shown in Figure 2.1. Essential parts of this equipment includes two Ailes Micrometer Microscopes used to measure deflections at load points, six precision made Beggs clamps used to simulate restraint, and various sets of close tolerance distortion plugs used to induce negative and positive deflections at the restraint and at floating gage points.

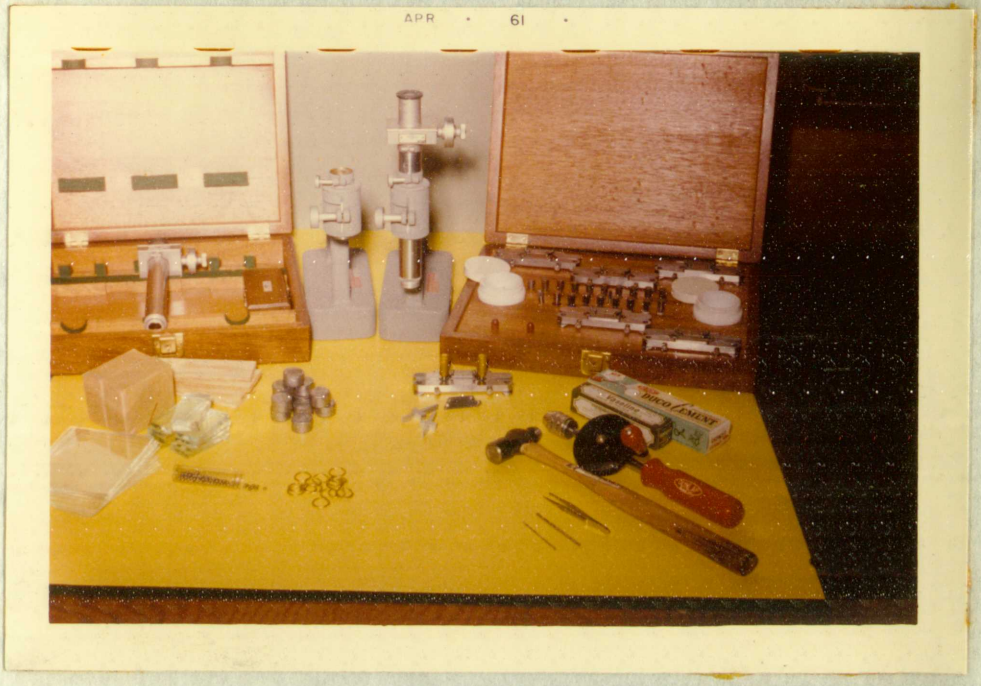

FIGURE 2

PHOTOGRAPH OF BEGGS DEFORMETER EQUIPMENT

The filar micrometer microscopes are quite sensitive in as much as readings as small as 39.37 micro inches can be read directly and readings can be estimated as small as 3.937 micro inches. This degree of refinement refers primarily to the micrometer rather than the setting of the cross-hairs on the target. It is difficult to position the cross-hairs on the same target twice with a variation of micrometer readings less than one division which represents 39.37 micro inches. Focusing and orienting of the microscope are done manually and cannot be done without the possibility of disturbing its position; therefore, making it essential that deflections toward and away from the microscope remain small. Refer to Figures 3 and 4 for a better understanding of the microscope and its operation.

The gage clamps shown in Figures 5 and 6 are composed of two accurately machined metal bars held together with cap screws and compression springs. One bar is accommodated with holes which permits its rigid attachment to a drawing board or other base while the second bar is movable which is used to support the model and to permit the inducement of known deflections by means of inserting different sets of

The filar micrometer microscopes are quite sensitive in as much as readings as small as 39.37 micro inches can be read directly and readings can be estimated as small as 3.937 micro inches. While design of reinforcement refers primarily to the micrometer rather than the setting of the cross-hairs on the target. It is difficult to position the cross-hairs on the same target twice with a variation of micrometer readings less than one division which represents 39.37 micro inches. Focusing and orienting of the microscope are done manually and cannot be done without the possibility of disturbing its position; therefore, making it essential that deflections toward and away from the microscope remain small. Refer to Figures 3 and 4 for a better understanding of the microscope and its operation.

The gage clamps shown in Figures 5 and 6 are composed of two accurately machined metal bars held together with cap screws and compression springs. One bar is accommodated with holes which permits its rigid attachment to a drawing board or other base while the second bar is movable which is used to support the model and to permit the insertion of known deflections by means of inserting different sets of

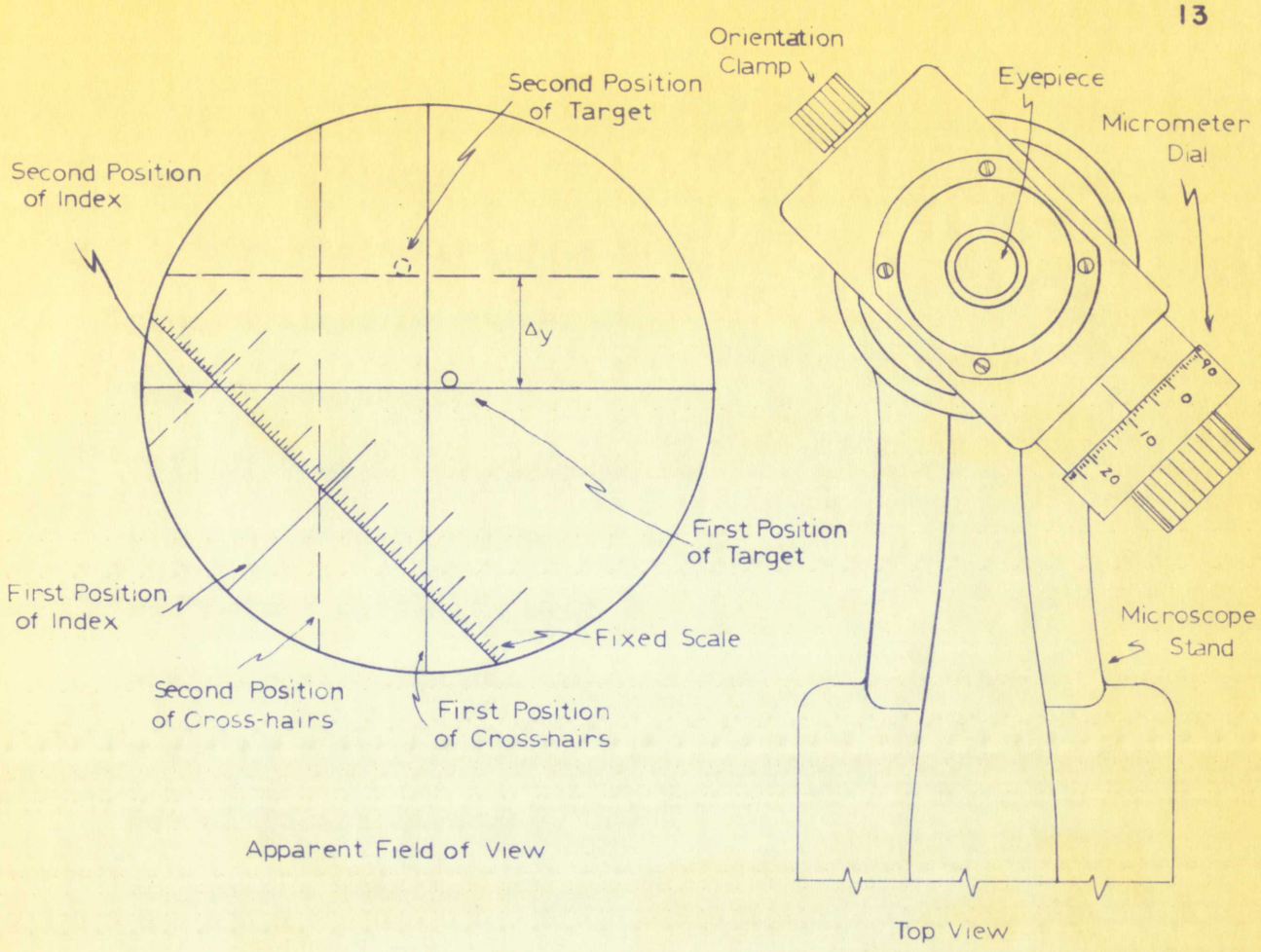

FIGURE 3 Micrometer Microscope

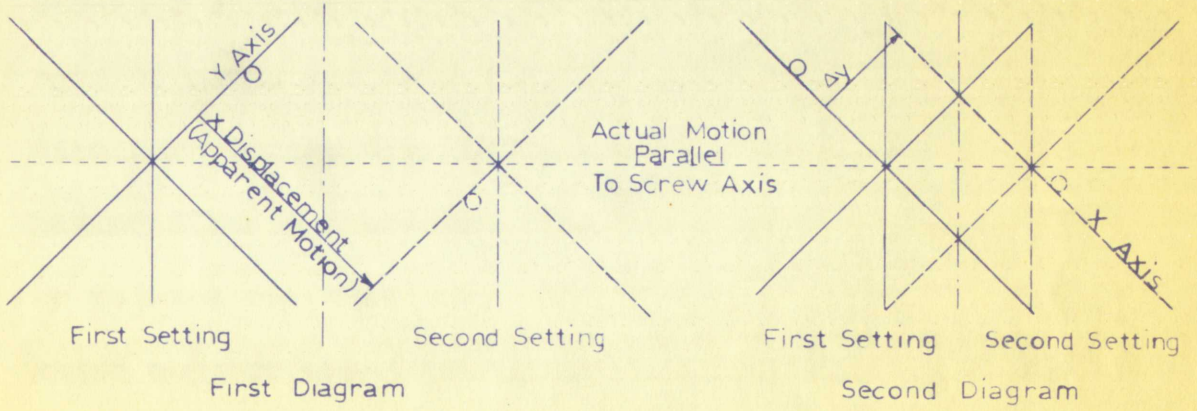

FIGURE 4 Micrometer Microscope Principle of Operation

distortion plugs.

The distortion plugs are machined to a tolerance of plus or minus two one-hundred-thousandths inches and are used in conjunction with the gage clamps to produce known deflections at the position of the clamp as shown in Figure 5. Five sets of distortion plugs are used in all. One set of "normal plugs" is used for each clamp remaining in position at all times when no distortions are being produced at that particular clamp. The "moment plugs" are of two different diameters and their positions are interchanged to produce rotation of the support without introducing any translation at the same time.

"Thrust plugs" are provided to introduce translation of the member attached to the gage clamp in a direction parallel to the axis of the member when the member is attached at right angles to the bars of the clamp. Two sets of plugs are used for this purpose, one set having diameters larger than the normal plugs and the other set having diameters smaller than the normal plugs. It should be pointed out that the clamp should be arranged as a pin ended support when the thrust plugs and shear plugs are

distortion plugs.

The distortion plugs are mounted to a tolerance of plus or minus two one-hundred-thousandths inches and are used in conjunction with the gage clamps to produce known deflections at the position of the clamp as shown in Figure 5. Five sets of distortion plugs are used in all. One set of "normal plugs" is used for each clamp remaining in position at all times when no distortions are being produced at that particular clamp. The "nonest plugs" are of two different diameters and their positions are interchanged to produce rotation of the support without introducing any translation at the same time.

"Thrust plugs" are provided to introduce translation of the member attached to the gage clamp in a direction parallel to the axis of the member when the member is attached at right angles to the bore of the clamp. Two sets of plugs are used for this purpose, one set having diameters larger than the normal plugs and the other set having diameters smaller than the normal plugs. It should be pointed out that the clamp should be arranged as a pin ended support when the thrust plugs and floor plugs are

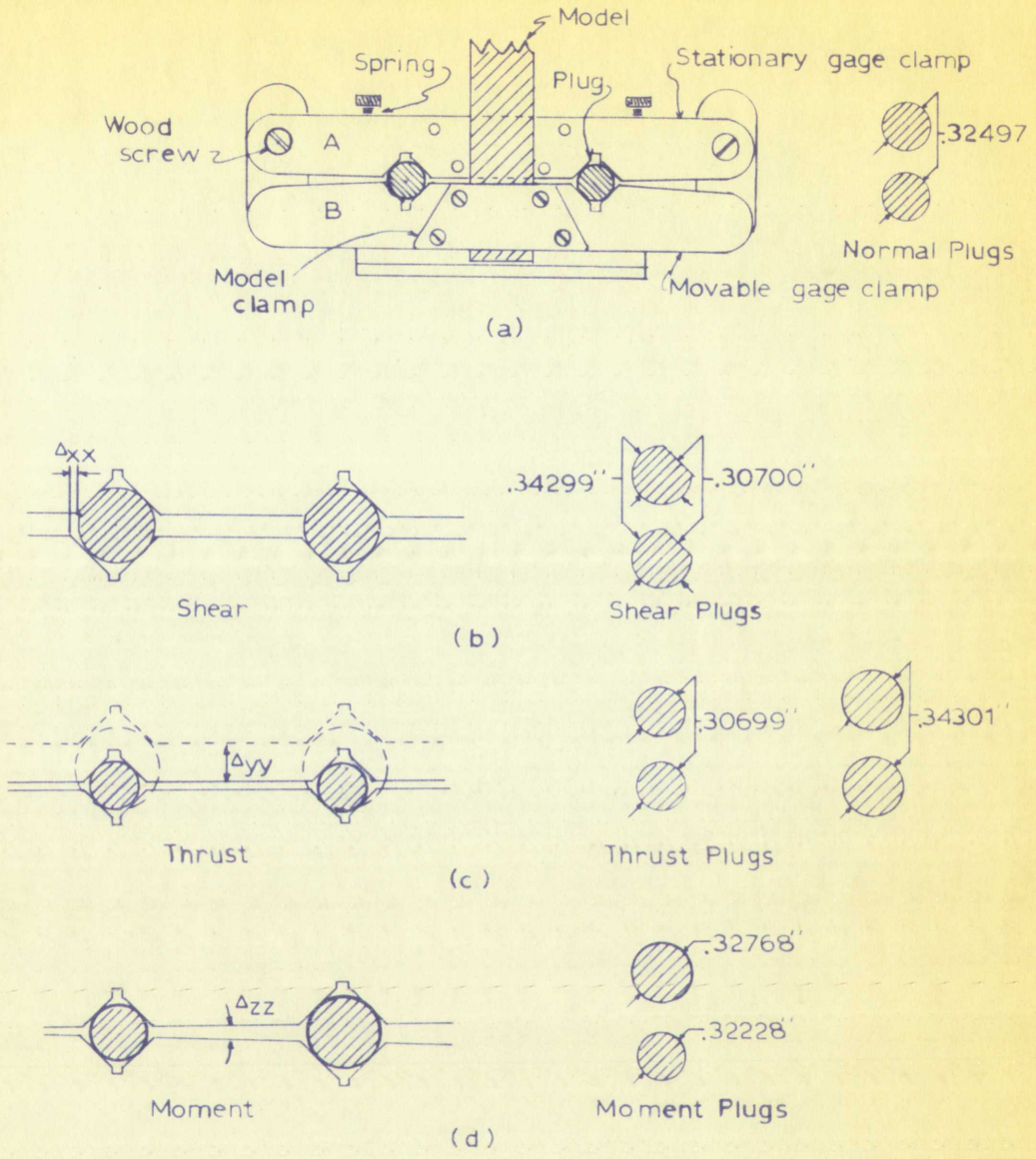

FIGURE 5 Deformeter Gage Clamp and Distortion Plugs

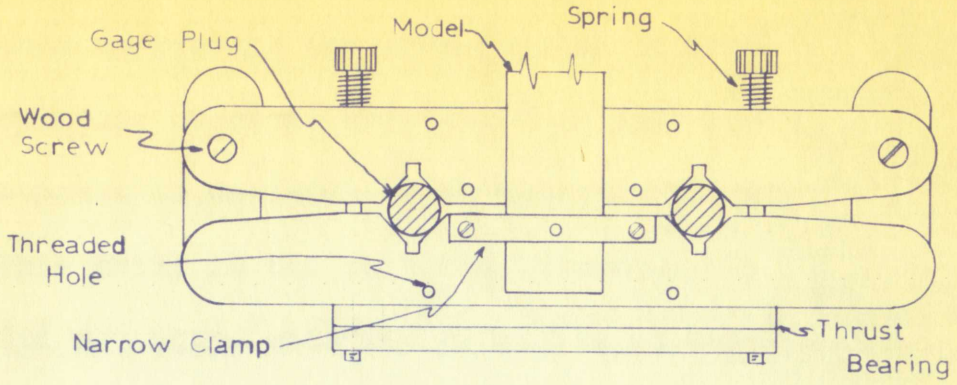

Mounted As A Pinned End

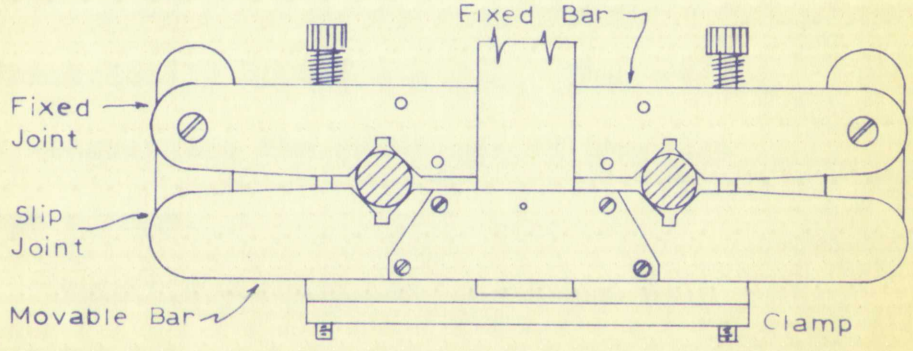

Mounted As A Fixed End

FIGURE 6 Pinned End and Fixed End Gage Conditions

used to prevent the introduction of moment at the support by means of chord rotation when only translation of the support is desired. Some experimentalists have overlooked this point in the past and, consequently, their solutions did not agree with the principle of superposition which is necessary for valid solutions.

"Shear plugs' are used to produce translation of the member at the gage clamp parallel to the bars of the clamp. These plugs are basically round with two flat surfaces on diametrically opposite sides. The translation is produced by rearranging the positions of the flat surfaces in the gage clamps.

Auxiliary equipment furnished with the apparatus includes spare parts for the gage assemblies, tools for mounting the clamps to a base such as a drafting board and for mounting models on the clamps. Also, lead weights, ball bearings, and pieces of plate glass are issued with the apparatus for stabilizing the models and for the making of various types of supports.

Different types of cutting tools were essential for model construction. Various hand saws were tried for cutting

need to prevent the introduction of moment at the support by means of shear reaction when only translation at the support is desired. Some experimentalists have overlooked this point in the past and, consequently, their solutions did not agree with the principle of superposition which is necessary for valid solutions.

"Shear plugs" are used to produce translation of the member at the gage clamp parallel to the plane of the clamp. These plugs are basically round with two flat surfaces at diametrically opposite sides. The translation is produced by restraining the positions of the flat surfaces in the gage clamps.

Auxiliary equipment furnished with the apparatus includes spare parts for the gage assemblies, tools for mounting the clamps to a base and as a drafting board and for mounting models on the clamps. Also, lead weights, ball bearings, and pieces of plate glass are issued with the apparatus for stabilizing the models and for the making of various types of supports.

Different types of casting resin were procured for model construction. Various hard resin were tried for bonding

the different model elements; however, it was found that electric powered band saws and sanding belts were ideal in preparation of the straight plastic model elements. Scales, callipers, scribes, and straight edges were of great help in sizing the members. Several types of cements were tried before a suitable kind was selected for joint construction. Cements are discussed further in connection with experimental procedures.

Wood blocking was secured to a drafting board for mountings of the various arrangements of the gage clamps. The drafting board was then supported on concrete blocks with bricks and additional concrete blocks placed on top of the board to weight it down sufficiently to prevent its inadvertent shifting. The microscope and model were supported on separate bases; hence, any inadvertent movement of either base could have resulted in erroneous readings. However, repeated readings were taken until consistency was observed.

the different model elements; however, it was found that an electric powered hand saw and sanding drill were useful in preparation of the straight plastic model elements. Scales, calipers, scribes, and straight edges were of great help in sizing the members. Several types of cements were tried before a suitable kind was selected for joint construction. Cements are discussed further in connection with experimental procedures.

Wood blocking was secured to a drafting board for mounting of the various arrangements of the gage clamps. The drafting board was then supported on cement blocks with bricks and additional concrete blocks placed on top of the board to weight it down sufficiently to prevent its inadvertent shifting. The microscope and recoil mass supported on separate bases; hence, any inadvertent movement of either base could have resulted in erroneous readings. However, repeated readings were taken until consistency was observed.

CHAPTER IV

EXPERIMENTS AND RESULTS

I. GENERAL

Several sequential steps were followed in obtaining experimental solutions to the problems chosen for this thesis. These steps consist of (1) calibrating the filar micrometer microscopes, (2) selecting model materials, (3) determining model scales, (4) constructing and installing models, (5) collecting and processing experimental data, (6) computing results, and (7) arranging the results for the report. Each of these items is discussed in considerable detail in this chapter.

Calibration

Two methods are commonly employed to calibrate the filar micrometer microscopes. First, when it is desirable to know the relationship between micrometer units and certain other units of length, such as inches, one has only to place a scale with the desirable units in the field of focus of the microscope and move the cross-hairs a distance of one unit on said scale while observing the change in micrometer units. Then, the deflections introduced by means

CHAPTER IV

EXPERIMENTAL PROCEDURE

A. GENERAL

Several sequential steps were followed in executing experimental solutions to the problems chosen for this thesis. These steps consist of: (1) calibrating the filar micrometer microscope, (2) selecting model materials, (3) determining model scales, (4) constructing and testing models, (5) collecting and processing experimental data, (6) computing results, and (7) writing the results for the report. Each of these items is discussed in considerable detail in this chapter.

Calibration

Two methods are commonly employed to calibrate the filar micrometer microscope. First, when it is desired to know the relationship between micrometer units and certain other units of length, such as inches, one may simply place a scale with the desirable units in the field of focus of the microscope and move the cross-hairs a different of one unit on said scale while observing the change in micrometer units. Then, the desired units introduced by means

of the gage clamps and distortion plugs are determined by observing the difference in diameters of the various distortion plugs.

Since a ratio of deflections is all that is necessary to satisfy the theoretical principles used with the Beggs method, there was no need for determining the relationship between micrometer units and inches. However, it was desirable to determine the amount of displacement produced at the gage clamps in terms of micrometer units for each manipulation of the three types of distortion plugs. This was done by placing a target on one of the clamps mounted on a drawing board then observing the amount of deflection produced by interchanging the various sets of distortion plugs.

In order to show the relationship of this deflection in the form of a calibration factor, reference is made to Müller-Breslau's principle as stated in Chapter II. This principle may be expressed in equation form as

$$R \triangle_2 = (1) \triangle_1 \qquad (2)$$

where the right side of equation represents a unit load applied at any desirable load point with $_1$ being the

of the dage clamps and distortion plugs are determined by observing the difference in diameters of the various distortion plugs.

Since a ratio of deflections is all that is necessary to satisfy the theoretical principles used with the Hegga method, there was no need for determining the relationship between micrometer units and inches. However, it was desirable to determine the amount of displacement produced at the dage clamps in terms of micrometer units for each manipulation of the three types of distortion plugs. This was done by placing a target on one of the clamps mounted on a drawing board then observing the amount of deflection produced by interchanging the various sets of distortion plugs.

In order to show the relationship of this deflection in the form of a calibration factor, reference is made to Muller-Breslau's principle as stated in Chapter IX. This principle may be expressed in equation form as

$$R \triangle_2 = (1) \triangle_1 \qquad (2)$$

where the right side of equation represents a unit load applied at any desirable load point with $_1$ being the

deflection of the structure at the load point caused by the unit load and being measured in the same direction as the line (or axis) of action of the unit load. On the left side of the equation, R represents the stress element caused at a different point on the structure by the unit load just described and $\triangle_2$ is the deflection that would occur at the position of R along the same line (or axis) of action of R if R were released. Equation (2) may be solved for R to yield

$$R = \frac{\triangle_1}{\triangle^2}(1). \qquad (3)$$

In the experimental solutions of the example problems in this chapter, $\triangle_2$ is the deflection induced at the gage clamps which is a constant for each set of distortion plugs. This permits a calibration factor equal to the unit load divided by $\triangle_2$. Equation (3) now becomes

$$R = CF(\triangle_1) \qquad (4)$$

where CF is the calibration factor and $\triangle_1$ is the measured deflection at the load point. It is obvious from equation (3) that the units used in measuring the deflections is immaterial provided $\triangle_1$ and $\triangle_2$ are expressed in like units.

deflection of the structure at the load point caused by the unit load and being measured in the same direction as the line (or axis) of action of the unit load. On the left side of the equation, R represents the stress element caused at a different point on the structure by the unit load just described and Δ_2 is the deflection that would occur at the position of R along the same line (or axis) of action of R if R were released. Equation (2) may be solved for R to yield

$$R = \frac{\Delta_1}{\Delta_2}(1). \qquad (3)$$

In the experimental solutions of the example problems in this chapter, Δ_2 is the deflection induced at the gage clamps which is a constant for each set of distortion plugs. This permits a calibration factor equal to the unit load divided by Δ_2. Equation (3) now becomes

$$R = CF(\Delta_1) \qquad (4)$$

where CF is the calibration factor and Δ_1 is the measured deflection at the load point. It is obvious from equation (3) that the units used in measuring the deflections is immaterial provided Δ_1 and Δ_2 are expressed in like units.

Calibration factors for the two microscopes used are shown in Table 1 below.

TABLE 1

CALIBRATION FACTORS

Distortion Plug	Microscope #221	Microscope #223
Moment	$\frac{1}{256}$	$\frac{1}{256}$
Shear	$\frac{1}{1287}$	$\frac{1}{1295}$
Thrust	$\frac{1}{1285}$	$\frac{1}{1289}$

Calibration factors are slightly different for different microscopes. Also, some variations may exist between calibrations performed by different persons; therefore, each observer should determine a particular set of calibration factors.

Selection of Model Materials

Factors governing the selection of model materials included (1) ease in fabrication, (2) mechanical properties, and (3) availability. Several plastic materials were considered that had similar mechanical properties in regards

Calibration factors for the two microscopes used are shown in Table I below.

TABLE I

CALIBRATION FACTORS

Dispersion Plug	Microscope #221	Microscope #313
Moment	$\frac{1}{256}$	$\frac{1}{250}$
Shear	$\frac{1}{1207}$	$\frac{1}{1235}$
Thrust	$\frac{1}{1285}$	$\frac{1}{1313}$

Calibration factors are slightly different for different microscopes. Also, some variation may result between calibrations performed by different persons therefore, each observer should determine a particular set of calibration factors.

Selection of Model Material

Factors governing the selection of model material included (1) ease in fabrication, (2) dimensional stability and (3) availability. Several plastic materials were considered that had adequate mechanical properties in strength

structural requirements. Also, the ease of fabrication of the different plastic materials was not greatly different. Steel splines were given close consideration because of their similarity with the materials commonly used in full sized structures. Also, rigid joints are easily obtained at the intersections of steel members by welding. However, it was decided that the forces necessary at the gage clamps to produce the desired deflections in steel models would be sufficiently large to endanger the rigidity of the clamps. Consequently, Kodapak[a], a transparent plastic material which was readily available at low cost was chosen for the structural elements of the models. One undesirable property of Kodapak is its low elastic modulus which would tend to magnify an instability condition. Problems of instability are discussed later in this chapter.

Different kinds of cement were experimented with to determine which was most favorable for use in joint connections. Both acetone and a mixed solution of acetone and ethylene dichloride were used in an effort to fuse weld the joints together with very little success. The fusion action

---

[a]Properties of Kodapak are listed in the appendices.

structural requirements. Also, the ease of fabrication of the different plastic materials was not greatly different. Steel splines were given close consideration because of their similarity with the materials commonly used in full sized structures. Also, rigid joints are easily obtained at the intersections of steel members by welding. However, it was decided that the forces necessary at the edge clamps to produce the desired deflections in steel models would be sufficiently large to endanger the rigidity of the clamps. Consequently, Kodapak®, a transparent plastic material which was readily available at low cost was chosen for the structural elements of the models. One undesirable property of Kodapak is its low elastic modulus which would tend to magnify an instability condition. Problems of instability are discussed later in this chapter.

Different kinds of cement were experimented with to determine which was most favorable for use in joint connections. Both acetone and a mixed solution of acetone and ethylene dichloride were used in an effort to fuse well the joints together with very little pressure. The mixed solution

---

®Properties of Kodapak are listed in the Appendix.

was quite easily produced, but the resulting joints were of a semi-plastic condition thereby giving hardly any similarity to rigid connections which were desired. Duco Household Cement #6241, Carter's Power Model Cement #470, and Eastman's #910 Cement were also tried without success. The first two of these spalled off after drying and bond could not be obtained with the latter. However, the recommended shelf life for the Eastment cement had expired by approximately eighteen months; therefore, it was not used because another supply was not readily available.

Carter's Vinyl Cement #469 proved to be adequate by permitting approximately forty-eight hours for curing. In addition to the long curing time required, it was necessary to take readings as soon as possible after inducing deflections to avoid appreciable error because of joint creep. This time interval was not long enough to permit the reading of both microscopes for any one particular distortion. Furthermore, it was often necessary to insert the wedges used to open the clamps for periods of time ranging from one to two minutes several times just prior to the reading

of the micrometer. This entailed (1) making an approximate setting of the cross-hairs on the target, (2) inserting the wedges into the clamp for one to two minutes, (3) removing the wedges from the clamp while observing the movement of the target. If the target was not exactly aligned with the cross-hairs at the instant the wedges were removed, the cross-hairs were readjusted and another trial was made.

II. THE SIGN PROBLEM

Problem Introduction

The first problem selected for experimental solution consisted of a sign stanchion built as a rigid frame bent with an overhanging arm to support a sign. In an effort to determine the effect that instability may have, if any, upon solutions by the Beggs method, members for the columns as shown in Figures 7, 8 and 9 were first selected with a slenderness ration of 672 which is 5.6 times that permitted in main steel columns of buildings. [13]

Since no loads were actually applied at the load point, indicated on the model as E, one may think that column instability would not enter into the experimental solutions.

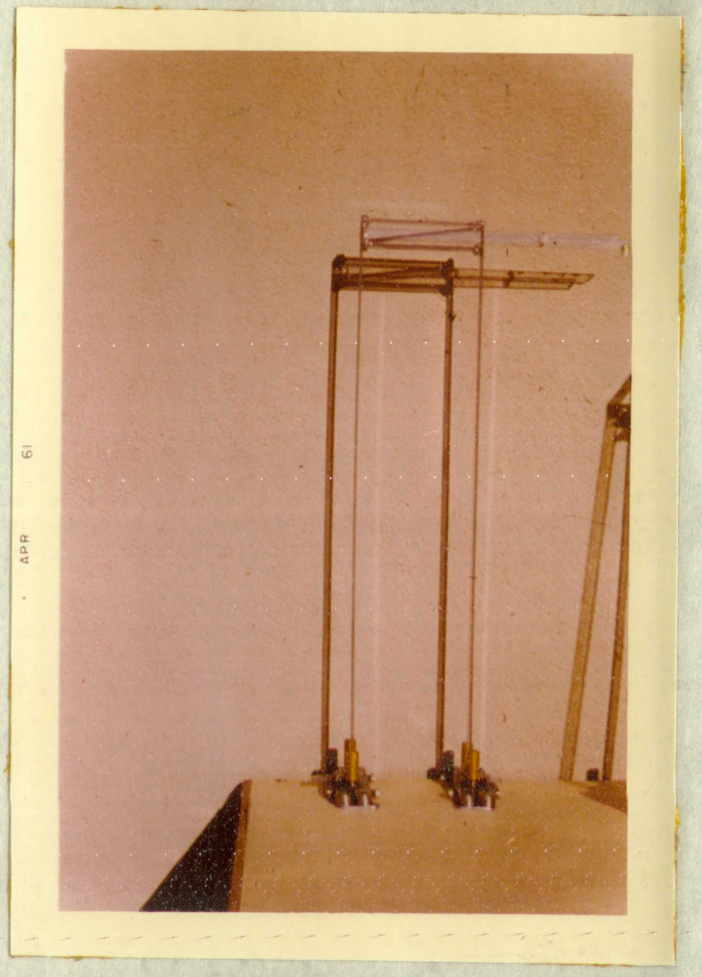

FIGURE 7

PHOTOGRAPH OF UNSTABLE SIGN STANCHION MODEL

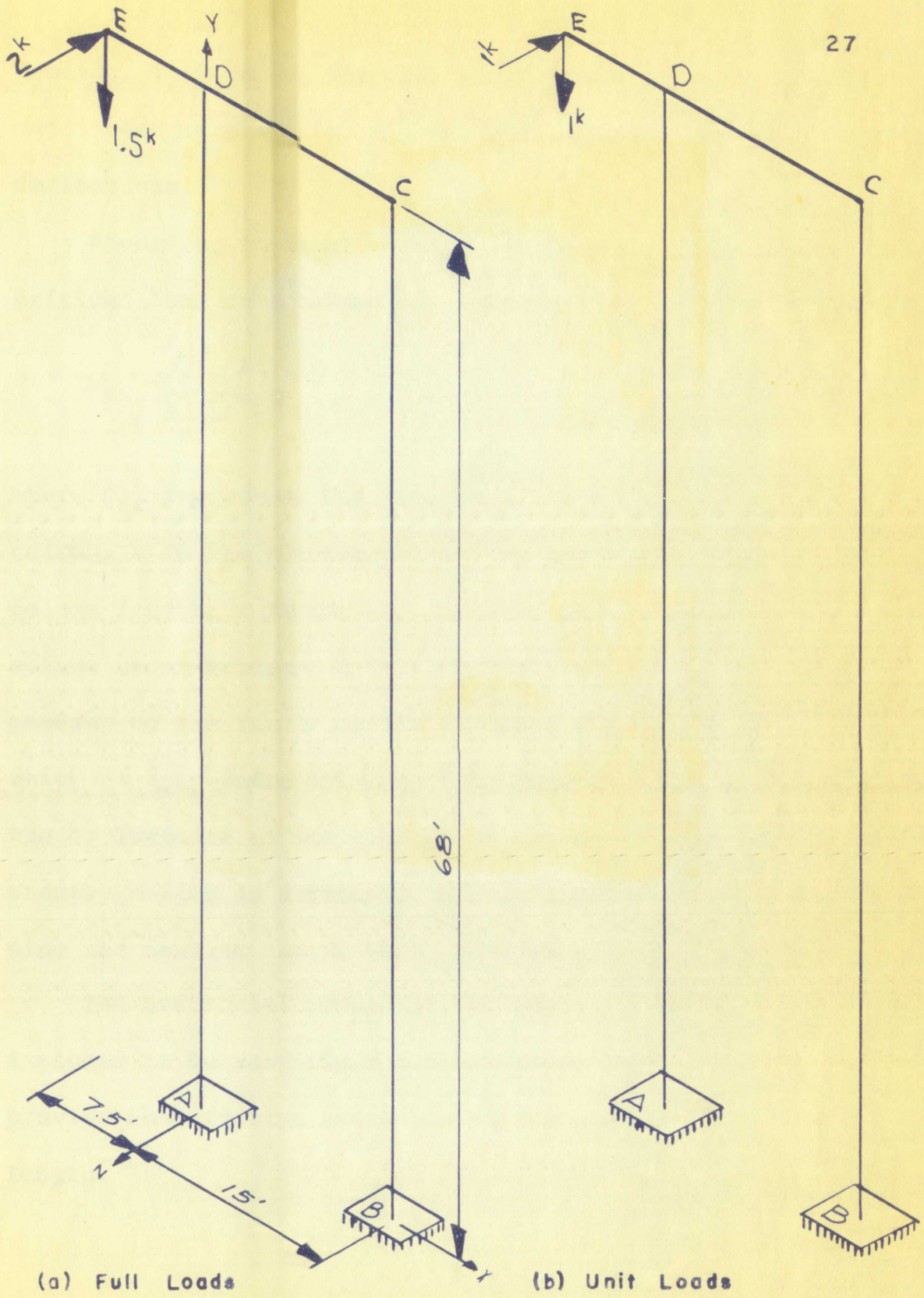

(a) Full Loads (b) Unit Loads

FIGURE 8

LOADING CONDITIONS AND DIMENSIONS OF UNSTABLE SIGN STANCHION

However, this is not the case since loads of certain magnitudes were applied at the gage clamps to produce the deflections.

According to Euler's theory on pin-ended columns, the critical load of a column is given by

$$P_{cr} = \frac{\pi^2 E}{\left[\frac{k L}{r}\right]^2} \qquad (5)$$

where P_{cr} represents the load required to buckle the column; E is the elastic modulus of the material; L is the column length; r is the least radius of gyration of the column cross-section; k is an effective length factor depending on the fixity of the supports which is taken as unity for pin-ended columns. The load necessary to induce the deflections at the gage clamp was difficult to compute thereby making it difficult, if not impossible, to determine the maximum length that could be used for the columns.

The horizontal member at the top of the structure was designed to be very rigid in comparison to the columns to provide an effective length of column equal to the actual length.

However, this is not the case since loads of certain magnitudes were applied at the gage clamps to produce the deflections.

According to Euler's theory on pin-ended columns, the critical load of a column is given by

$$P_{cr} = \frac{\pi^2 E I}{\left[\frac{k L}{r}\right]^2} \qquad (5)$$

where P_{cr} represents the load required to buckle the column; E is the elastic modulus of the material; L is the column length; r is the least radius of gyration of the column cross-section; k is an effective length factor depending on the fixity of the supports which is taken as unity for pin-ended columns. The load necessary to induce the deflections at the gage clamp was difficult to compute thereby making it difficult, if not impossible, to determine the maximum length that could be used for the column.

The horizontal member at the top of the structure was designed to be very rigid in comparison to the columns to provide an effective length of column equal to the actual length.

Procedure

A model scale of ½" = 1'-0" was chosen; then drawings of the model were made before any cutting of the material was started. Approximately one-half inch of material was provided as extensions to the columns for purposes of attaching the gage clamps while still permitting the entire column length to be measured above the gage clamp. The model pieces were then cut out and trimmed to size. This was accomplished by cutting the pieces slightly oversized with an electric powered band saw then sanding them to size with an electric sander. Small pieces of model material were cut to size and cemented to inside corners of the model joints in an effort to make the joints as rigid as possible thereby reducing cement creep at the joints. A photograph of the completed model is shown in Figure 7 and drawings showing model dimensions are shown in Figure 9. Structural dimensions and loading conditions are illustrated in Figure 8.

With the model having been built and arranged as described above, the supports at points A and B were then

Procedure

A model scale of 1" = 1'-0" was chosen; then drawings of the model were made before any cutting of the material was started. Approximately one-half inch of material was provided as extensions to the columns for purposes of attaching the gage clamps while still permitting the entire column length to be measured above the gage clamp. The model pieces were then cut out and trimmed to size. This was accomplished by cutting the pieces slightly oversized with an electric powered band saw then sanding them to size with an electric sander. Small pieces of model material were cut to size and cemented to inside corners of the model joints in an effort to make the joints as rigid as possible thereby reducing cement creep at the joints. A photograph of the completed model is shown in Figure 7 and drawings showing model dimensions are shown in Figure 9. Structural dimensions and loading conditions are illustrated in Figure 8.

With the model having been built and arranged as described above, the supports at points A and B were then

rotated about their respective x-axes by inserting the moment distortion plugs into the gage clamps and then reversing their first arrangements. To do this, the gage clamps were arranged similarly to that shown in Figure 10 for the stabilized sign stanchion.

Microscope #221 was arranged in a horizontal position, as shown also in Figure 10, to view an ink dot on a piece of white paper located at the load point E. This permitted measuring of deflections along lines of action of both the horizontal and vertical loads with a single microscope and without changing its orientation. After completing measurements related to the moments just described, the supports were then changed to represent pinned connections while vertical and horizontal displacements were produced by manipulating the thrust plugs and shear plugs respectively. Only one support being subjected to the various distortions was arranged as a pinned connection until measurements were complete for that support, then the support was re-fixed while translations were produced at the second support.

In order to provide a means of supporting the model

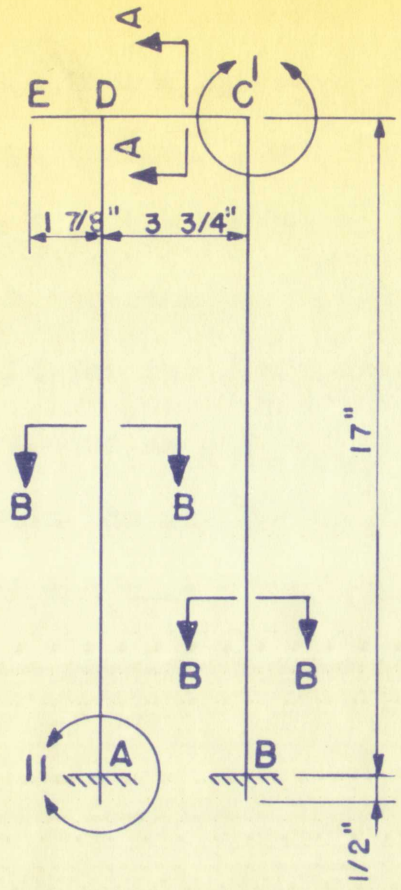

ELEVATION

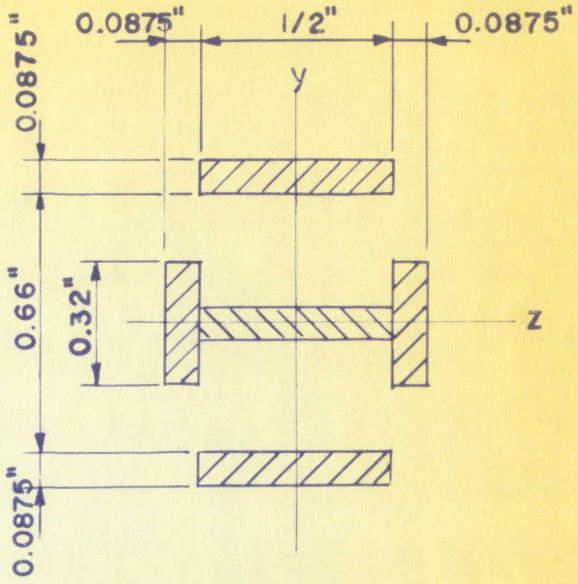

A – A

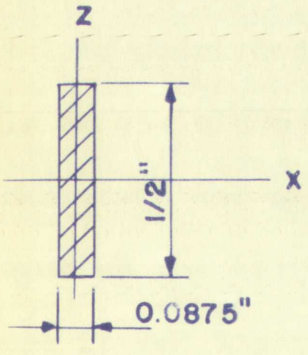

B – B

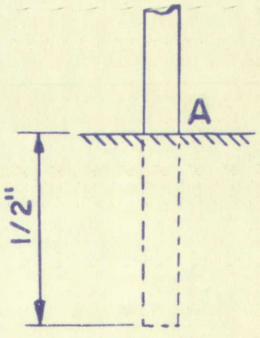

DETAIL II

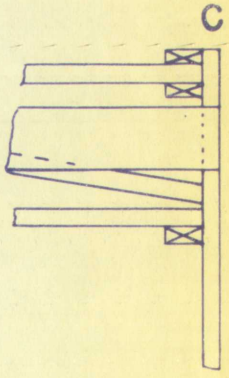

DETAIL I

FIGURE 9

MODEL DRAWINGS OF UNSTABLE SIGN STANCHION

in such a manner as to allow the inducement of rotation of the supports about their vertical axes, the excess material was cut from the column bases and replaced with "horizontal shoes" being cemented to the bases as shown in Detail I of Figure 14 for the stabilized model. The gage clamps were then arranged as shown in Figure 11 of the stabilized model. Here again the supports were fixed while rotation was being produced and then pinned for translations in the x-directions.

This problem was statically indeterminate to the sixth degree; hence, with four of the reaction components being determined from the above information, it was evident that the moments in the x-y plane could be determined by the methods of statics.

Difficulty was experienced in reading deflections when the load point deflected in a direction parallel to the axis of the microscope tube. The field of focus of the microscopes was small thereby giving slightly blurred images as the target neared the extremes of the focal range. Since it was impossible to change the focal range on the microscope without moving the entire instrument, possible

in such a manner as to allow the inducement of rotation of the supports about their vertical axes, the excess material was cut from the column bases and replaced with "horizontal spoke" being cemented to the bases as shown in Detail I of Figure 14 for the stabilized model. The page clamps were then arranged as shown in Figure 11 of the stabilized model. Here again the supports were fixed while rotation was being produced and then pinned for translations in the x-directions.

This problem was statically indeterminate to the sixth degree; hence, with four of the reaction components being determined from the above information, it was evident that the moments in the x-y plane could be determined by the methods of statics.

Difficulty was experienced in reading deflections when the load point deflected in a direction parallel to the axis of the microscope tube. The field of focus of the microscope was small thereby giving slightly blurred images as the target neared the extremes of the focal range. Since it was impossible to change the focal range on the microscope without moving the entire instrument, possible

errors due to observation of blurred images had to be tolerated.

The procedure described above for the unstable frame was again followed for the more stable frame shown in Figures 10, 11, 12, 13 and 14.

Analysis and Results

Computations required to transform experimental data into results were quite simple. The reactions caused by the unit loads were readily obtained by multiplying the right side of equation (4) by the scale factor. The scale factor for moment components amounted to the reciprocal of the model scale for each of the models used in this thesis, while the scale factor for force components is always unity regardless of the model scale. After computing unit load reactions and multiplying them by their respective load factors, the principle of superposition was used to determine the reactions caused by the combined total loading conditions. A comparison of experimental results with those obtained from simplified mathematical analysis often used for a basis of design of such structures is shown in

errors due to observation of plotted trends had to be
tolerated.

The procedure described above for the symmetric tests
was again followed for the more subtle trends shown in
Figures 10, 11, 12, 13 and 14.

Analysis and Results

Computations required to translate experimental data
into results were quite simple. The reaction caused by
the unit loads were readily obtained by multiplying the
right side of equation (4) by the scale factor. The scale
factor for moment components attached to the reciprocal of
the model scale for each of the moduli used in this tests,
while the scale factor for force components is simply unity
regardless of the model scale. After computing unit load
reactions and multiplying them by their respective load
factors, the principle of superposition was used to deter-
mine the reactions caused by the combined total loading
conditions. A comparison of experimental results with
those obtained from simplified mathematical analysis often
used for a basis of design of such structures is given in

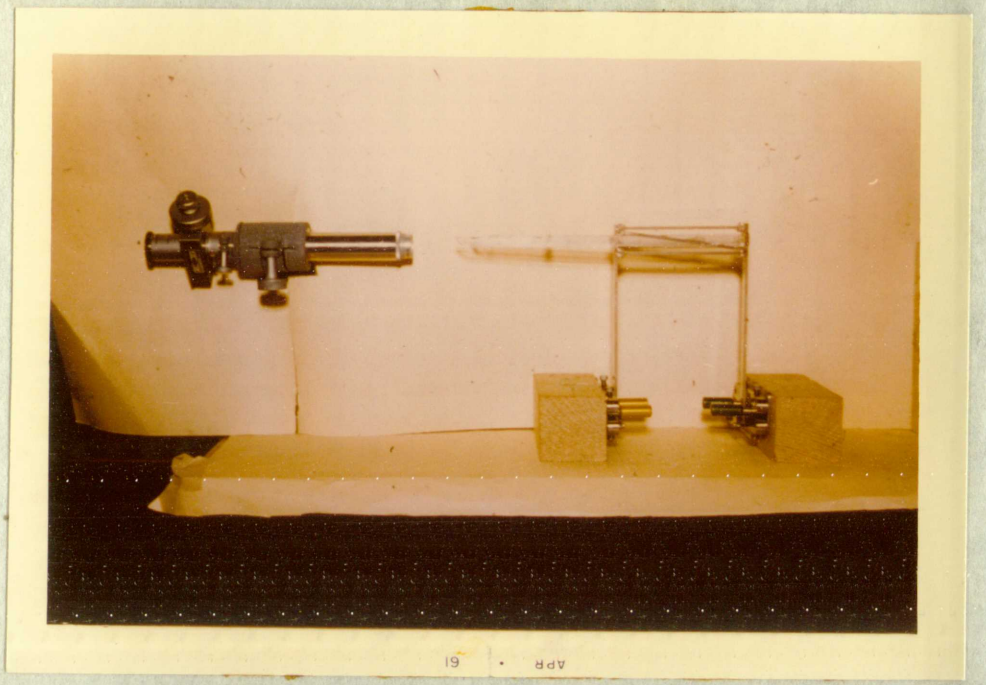

FIGURE 10

PHOTOGRAPH OF STABLE SIGN MODEL ARRANGED
FOR ROTATION OF SUPPORTS IN Y-Z PLANE

FIGURE 11

PHOTOGRAPH OF STABLE SIGN MODEL ARRANGED
FOR ROTATION OF SUPPORTS IN X-Z PLANE

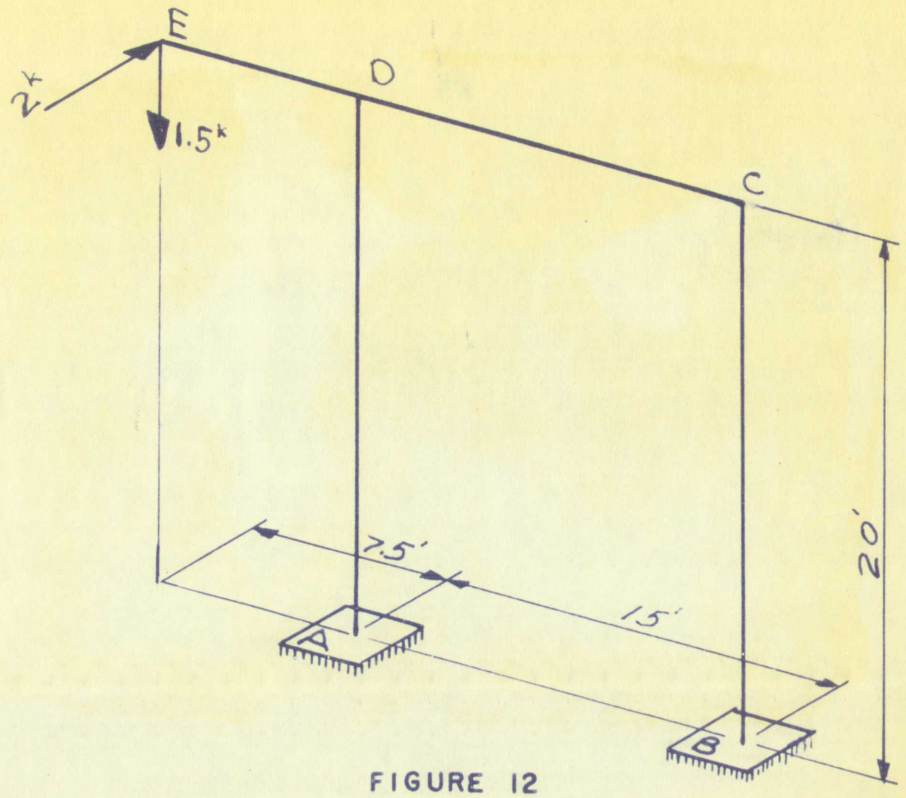

FIGURE 12

LOADING CONDITIONS AND DIMENSIONS OF STABLE SIGN STANCHION

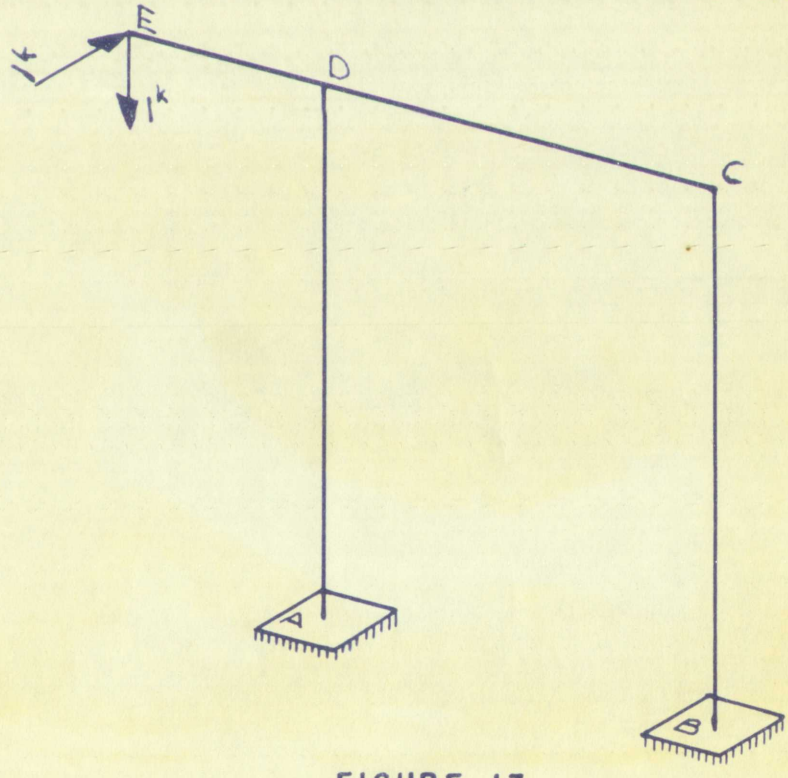

FIGURE 13

UNIT LOADING CONDITIONS OF STABLE SIGN STANCHION

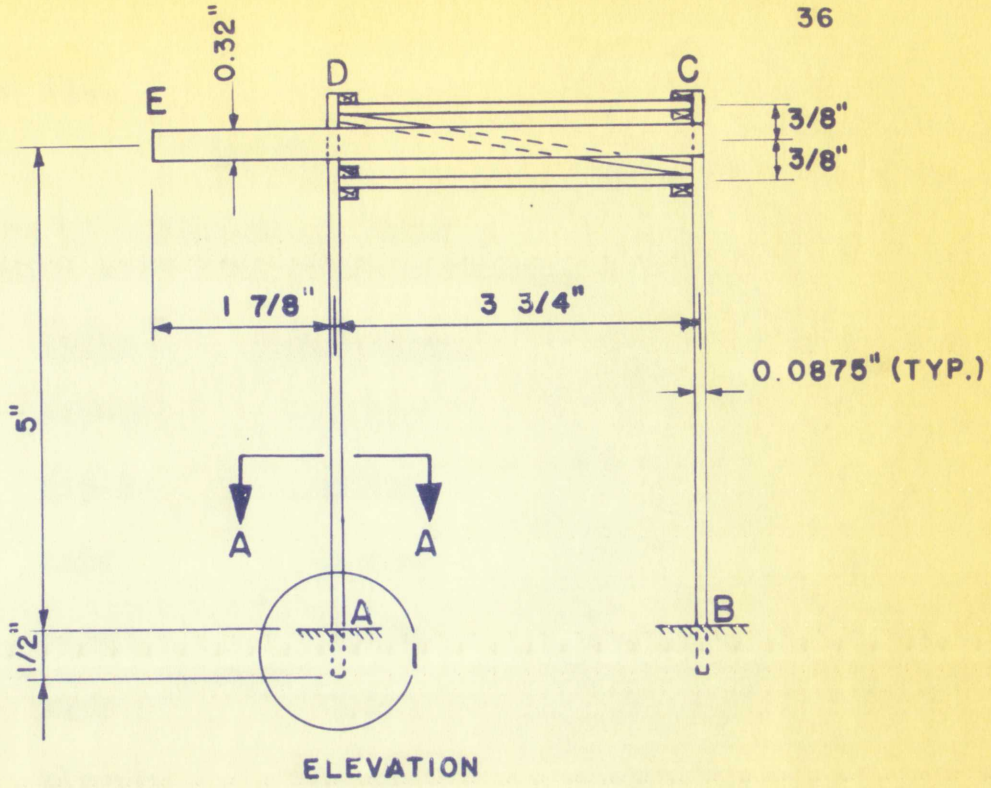

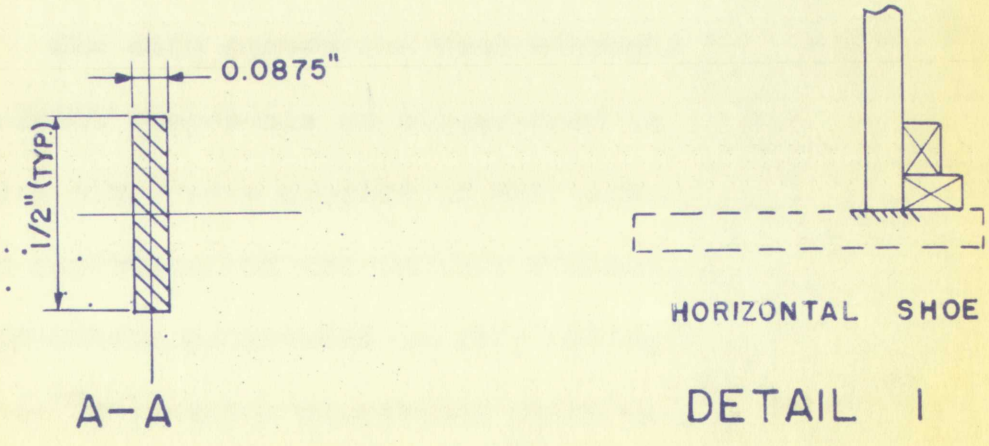

FIGURE 14

MODEL DRAWINGS OF STABLE SIGN STANCHION

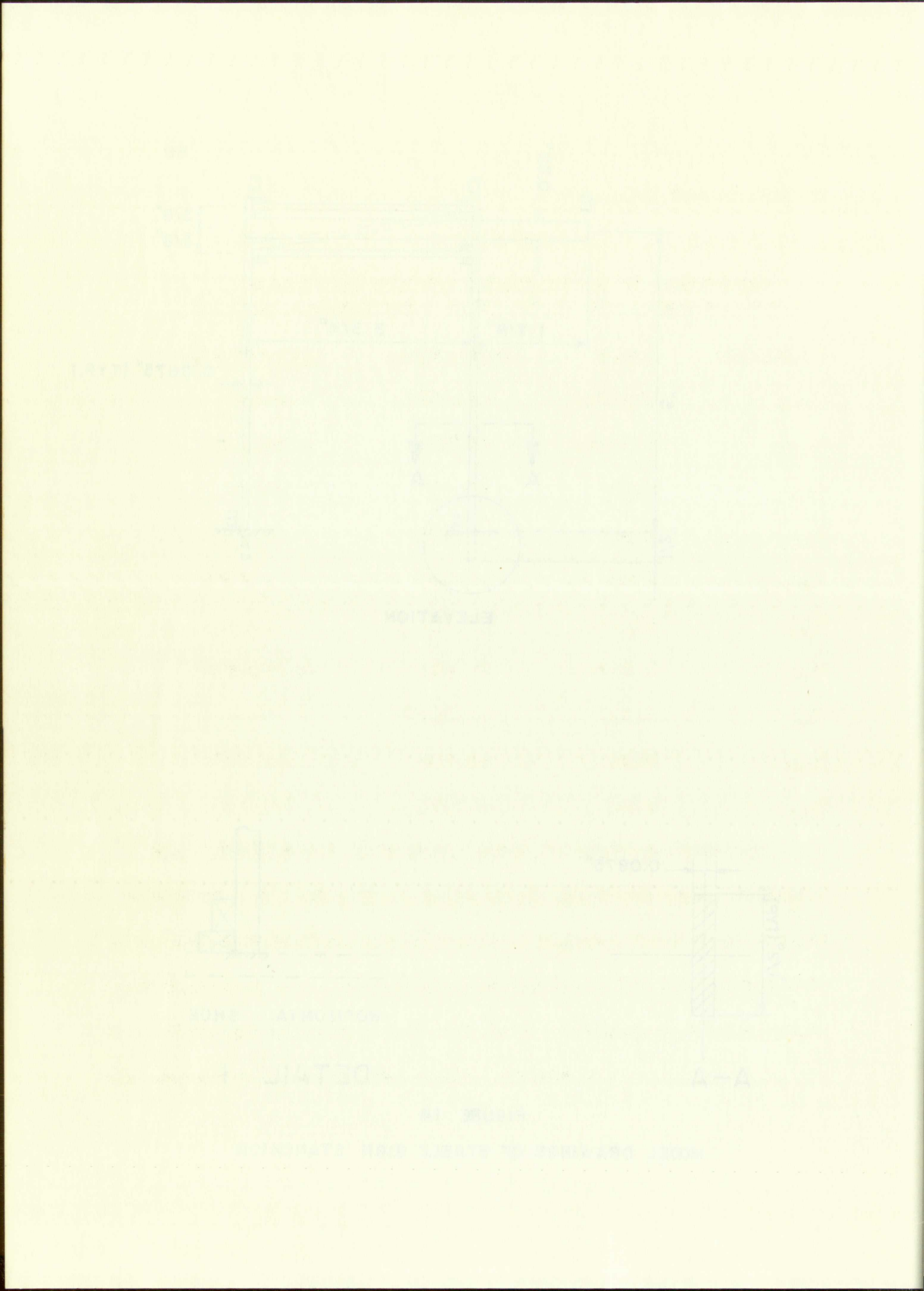

Tables II and III.

TABLE II

COMPARISON OF EXPERIMENTAL RESULTS FOR UNSTABLE SIGN STANCHION WITH SIMPLIFIED MATHEMATICAL RESULTS

Component	Units	Experimental	Mathematical
M_{Axz}	kip-ft.	-11.100	-----
M_{Ayz}	kip-ft.	-122.030	-204.000
R_{Ax}	kips	-0.009	-----
R_{Ay}	kips	2.262	2.250
R_{Az}	kips	0.299	3.000
M_{Bxz}	kip-ft.	-7.904	-----
M_{Byz}	kip-ft.	57.846	68.000
R_{Bx}	kips	-0.012	-----
R_{By}	kips	-0.756	-0.750
R_{Bz}	kips	-0.334	-1.000

The sign convention used throughout this thesis for reaction components is illustrated in Figure 15. No algebraic signs were applied to the various micrometer readings. The directions of the various deflections were noted as the experiments progressed thereby making possible the determination of reaction directions which were also recorded on the

Tables II and III.

data sheets.

TABLE III

COMPARISON OF EXPERIMENTAL RESULTS FOR STABLE SIGN STANCHION WITH SIMPLIFIED MATHEMATICAL RESULTS

Component	Units	Experimental	Mathematical
M_{Axz}	kip-ft.	- 3.776	------
M_{Ayz}	kip-ft.	-49.324	-60.000
R_{Ax}	kips	0.021	------
R_{Ay}	kips	2.248	2.250
R_{Az}	kips	2.537	3.000
M_{Bxz}	kip-ft.	- 3.122	------
M_{Byz}	kip-ft.	9.080	20.000
R_{Bx}	kips	- 0.010	------
R_{By}	kips	- 0.751	- 0.750
R_{Bz}	kips	- 0.542	- 1.000

The first letter of each component designates the type of stress element. M is used for moment components and R for force components. The capitalized subscript designates the location of the component. The lower case subscripts identify the plane or line of action of the component.

Table II illustrates the effects of instability on the

data sheets.

TABLE III

COMPARISON OF EXPERIMENTAL RESULTS FOR STRAIGHT STANCHION WITH SIMPLIFIED MATHEMATICAL THEORY

Component	Units	Experimental	Mathematical
M_{Xs}	kip-ft.	+ 3.778	------
M_{Ys}	kip-ft.	-43.324	-39.001
R_{Xs}	kips	0.021	------
R_{Ys}	kips	2.348	2.330
R_{Zs}	kips	3.537	3.000
M_{Xs}	kip-ft.	-3.131	------
M_{Ys}	kip-ft.	2.080	2.039
R_{Xs}	kips	- 0.010	------
R_{Ys}	kips	- 0.731	- 0.750
R_{Zs}	kips	- 0.542	- 1.000

The first letter of each component designates the type of stress element. M is used for moment components and R for force components. The capital subscript designates the location of the component. The next small subscript identify the plane or line of action of the component.

Table II illustrates the effect or insensitivity on the

experimental solution when compared further with solutions of equilibrium equations of statics for the entire structure. The mathematical solution agrees with conditions of static equilibrium because it was based on the validity of the equilibrium equations. However, the problem of instability was completely ignored in the mathematical solution.

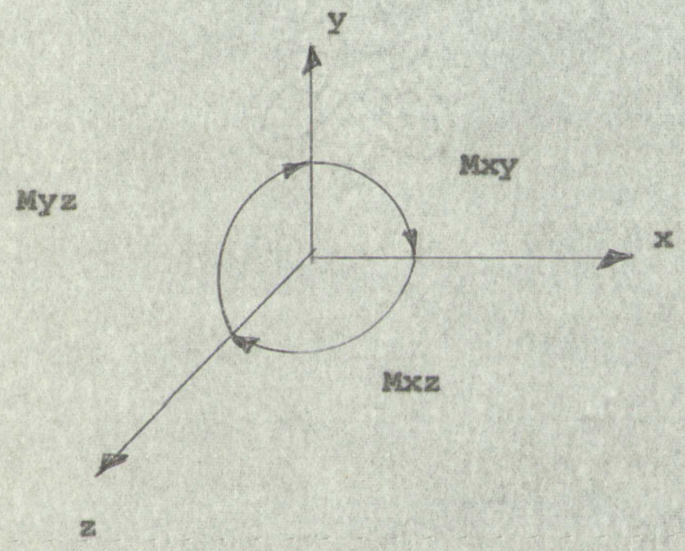

FIGURE 15

SIGN CONVENTION
(VECTORS SHOWN INDICATE POSITIVE DIRECTIONS)

The experimental results shown in Table III are in close agreement with the equilibrium conditions for the entire frame drawn as a free body diagram. Comparison of

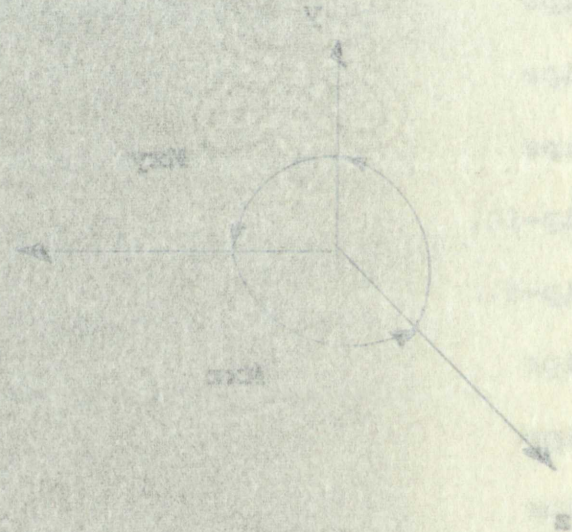
y
x
z

these results with the conditions of static equilibrium are shown in Table IV. The largest imbalance indicated by comparisons in Table IV is less than one-percent which indicates a very accurate experimental solution.

The mathematical results shown in Table III illustrates the crudeness of the mathematical analysis employed and points to inefficient designs based on such an analysis.

TABLE IV

COMPARISON OF EXPERIMENTAL RESULTS OF STABLE SIGN STANCHION WITH CONDITIONS OF STATIC EQUILIBRIUM

Component	Units	Experimental Reactions	External Loads	Imbalance	% Diff.
M_{xz}	kip-ft.	-14.936	15.000	0.064	0.427
M_{yz}	kip-ft.	-20.134	20.000	0.134	0.685
R_x	kips	0.026	0	0.026	-----
R_y	kips	1.497	- 1.500	0.003	0.231
R_z	kips	0.994	- 1.000	0.006	0.600

III. THE TOWER PROBLEM

Problem Introduction

The second problem chosen for experimental investigation

III. THE TOWER PROBLEM

Problem Introduction

The second problem chosen for experimental investigation

was a two wire transmission tower as shown in Figure 16. Normally, three or more transmission lines are carried by such towers; however, only two were simulated in the problem discussed here because only two microscopes were available for measuring deflections. The problem is not unusual; however, the design of such towers is usually based on greatly simplified mathematical analysis.

An effort was made to simulate fixed supports and fixed joints for representation of welded construction. In order to illustrate the complexity of a rigorous mathematical solution, it is pointed out here that one-hundred-fifty stress elements must be determined; hence, the problem is statically indeterminate to the one-hundred-forty-fourth degree. The use of any presently known mathematical method for a solution would require a great deal of work, even with the aid of an electronic computer. Also, it is pointed out that an experimental investigation necessary for the determination of every stress element in the structure would prove to be something more than a small task in itself even with the aid of properly designed equip-

was a two wire transmission tower as shown in Figure 1c. Normally, three or more transmission lines are carried by each tower; however, only two were simulated in the problem discussed here because only two strain-gages were available for measuring deflection. The problem is not unusual; however, the design of such towers is usually based on greatly simplified mathematical analysis.

An effort was made to simulate fixed supports and fixed joints for representation of welded connections. In order to illustrate the complexity of a rigorous mathematical solution, it is pointed out here that one-hundred-fifty stress elements must be determined; hence, the problem is statically indeterminate to the one-hundred-forty-fourth degree. The use of any presently known mathematical method for a solution would require a great deal of work, even with the aid of an electronic computer. Also, it is pointed out that an experimental investigation necessary for the determination of every stress element in the structure would prove to be something more than a small task in itself even with the aid of properly designed multi-

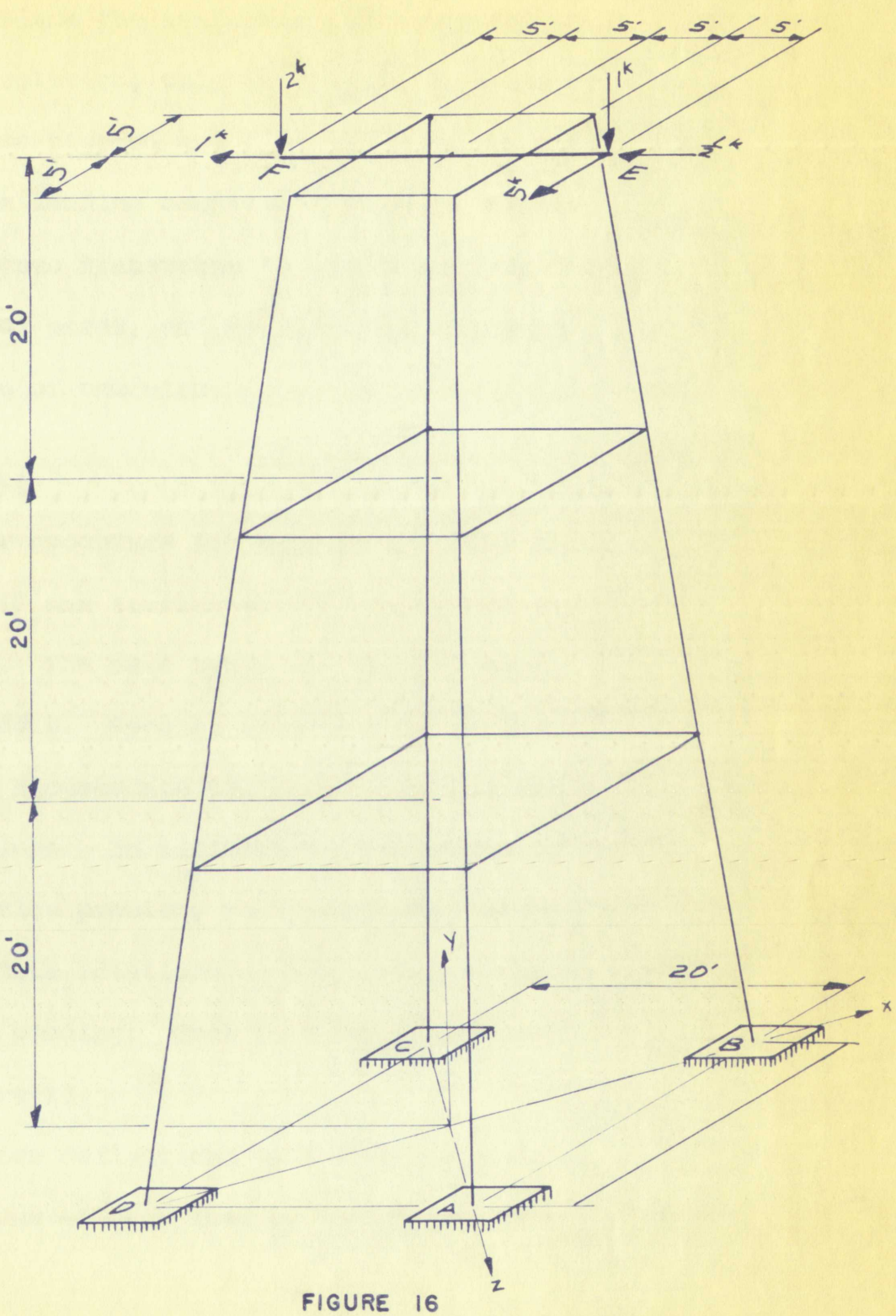

FIGURE 16

LOADING CONDITIONS AND DIMENSIONS OF TOWER STRUCTURE

ment. Since the available equipment was inadequate for such a solution, only the stress elements at the supports were investigated and illustrated in this thesis.

The loading conditions shown in Figure 16 represent wind forces transverse to the wires, ice on the wires, weight of wires, and an eccentric force caused by the collapse of one wire.

Procedure

The procedure for constructing the model shown in Figure 17 was similar to that described for the sign problem. The same types of model materials were used in both models. Special arrangements of the supports were made to accommodate the gage clamps in producing the desired deflections. In addition to the horizontal shoes described in the sign problem, vertical shoes were provided to accommodate rotations of the supports about their weak axis of bending. Such an arrangement is shown in Detail I of Figure 17.

Since deflections were measured in three different directions at each load point, it was necessary to rearrange

ment. Since the available equipment was inadequate for such a solution, only the stress elements at the supports were investigated and illustrated in this thesis.

The loading conditions shown in Figure 16 represent wind forces transverse to the wires, ice on the wires, weight of wires, and an eccentric force caused by the collapse of one wire.

Procedure

The procedure for constructing the model shown in Figure 17 was similar to that described for the sign problem. The same types of model materials were used in both models. Special arrangements of the supports were made to accommodate the gage clamps in producing the desired deflections. In addition to the horizontal shoes described in the sign problem, vertical shoes were provided to accommodate rotations of the supports about their weak axis of bending. Such an arrangement is shown in Detail I of Figure 17.

Since deflections were measured in three different directions at each load point, it was necessary to rearrange

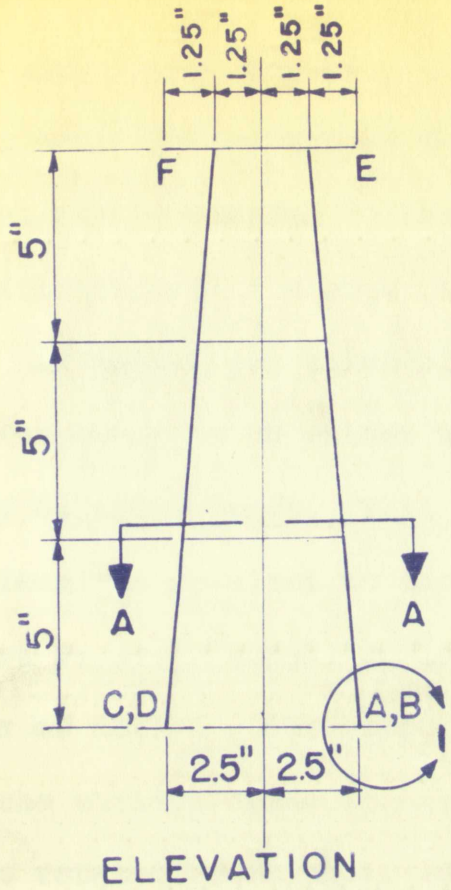

ELEVATION

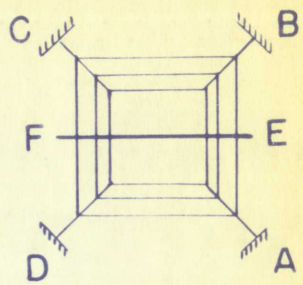

PLAN

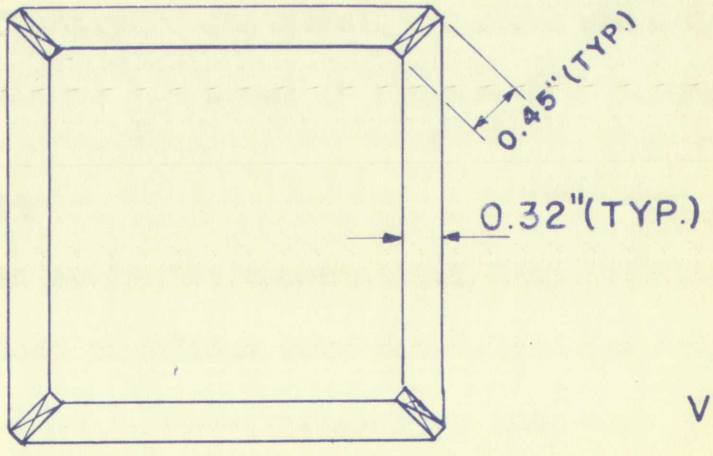

A–A

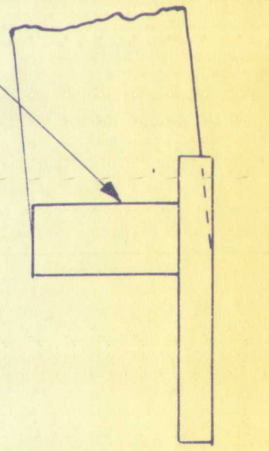

VERTICAL SHOE

DETAIL I

FIGURE 17

DRAWINGS OF TOWER MODEL

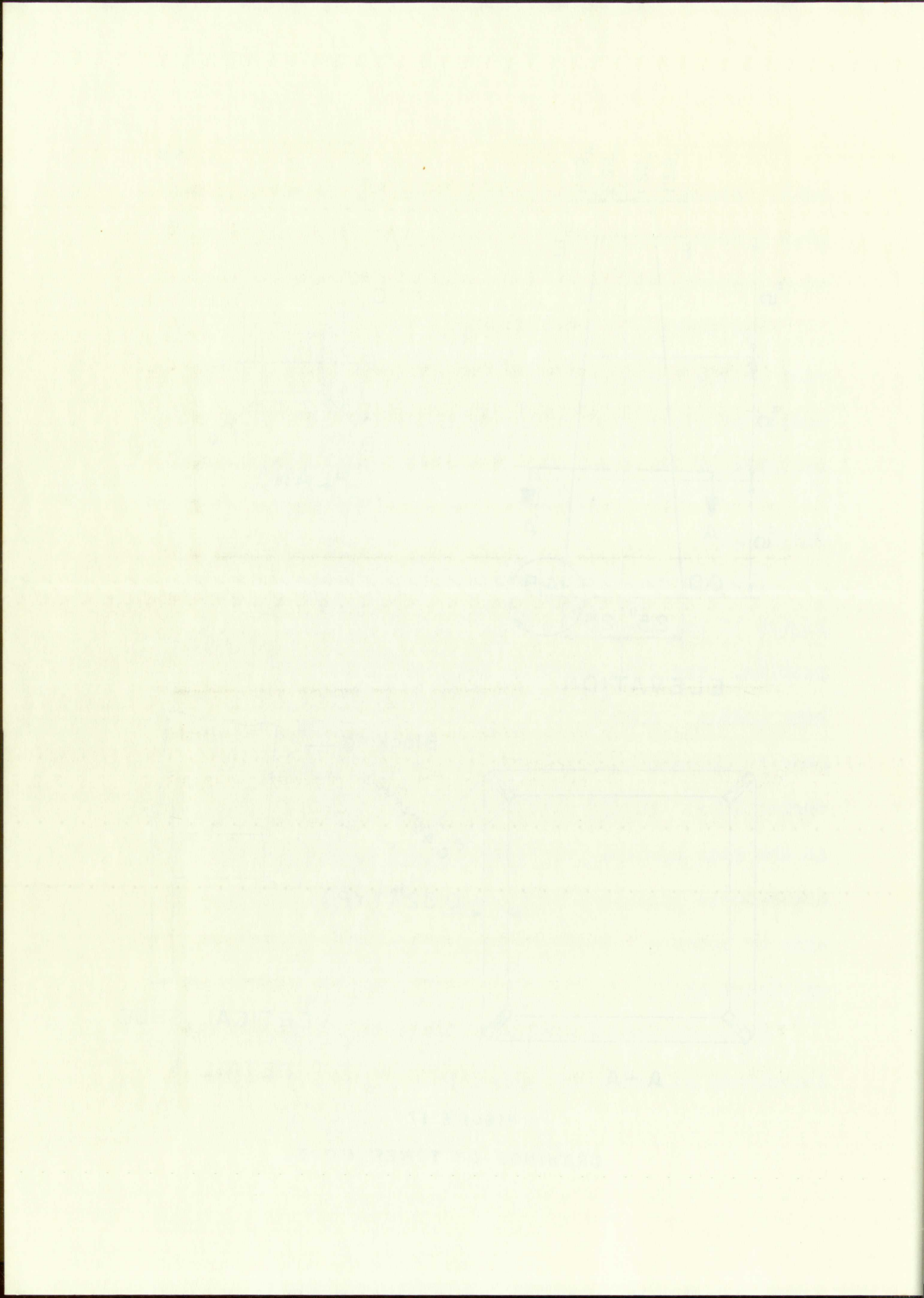

the microscopes for each arrangement of the gage clamps. This would not have been entirely necessary provided the model had not needed to have been revised for different orientations of the gage clamps.

Advantage was taken of the vertical axis of symmetry of the tower to an extent that deflections were induced only at one support. This was made possible by measuring deflections parallel to the transmission line at load point F; even though, no loads were indicated along that line of action. The support at A was used for inducement of the various deflections; however, all four supports were rotated about their vertical axes while the corresponding deflections were measured and compared to check the symmetry of the model. Various orientations of the gage clamps are shown in Figures 18, 19, and 20.

Results

In analysing experimental data for this problem, the unit load reactions were determined for the support at point A in a manner similar to that used in connection with the sign problem. In addition to the determination of

Results

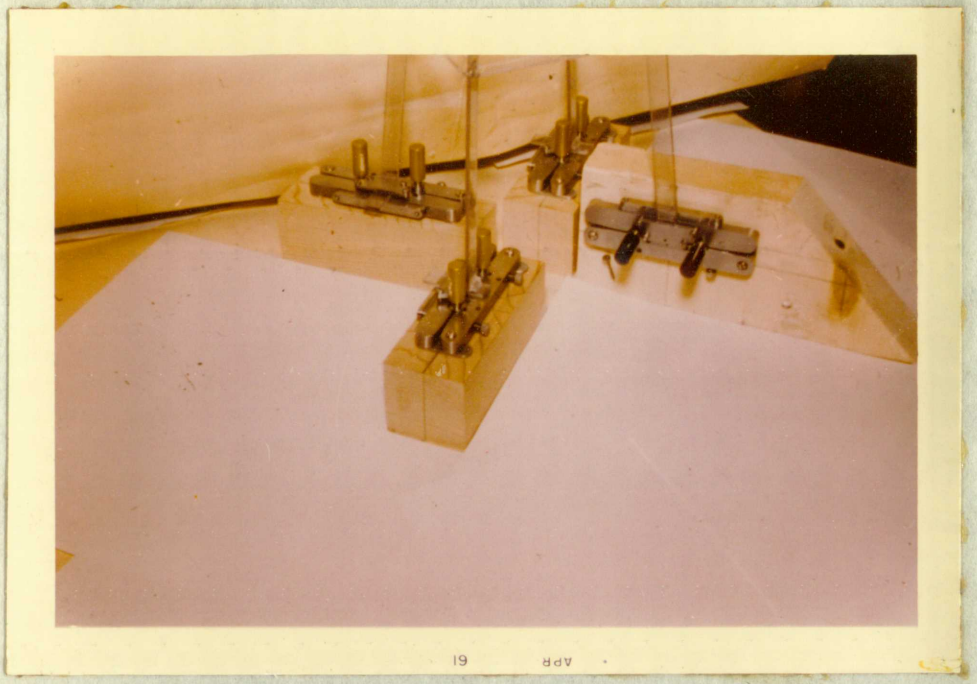

FIGURE 18

PHOTOGRAPH OF TOWER MODEL ARRANGED
FOR DISTORTIONS IN Y-Z PLANE

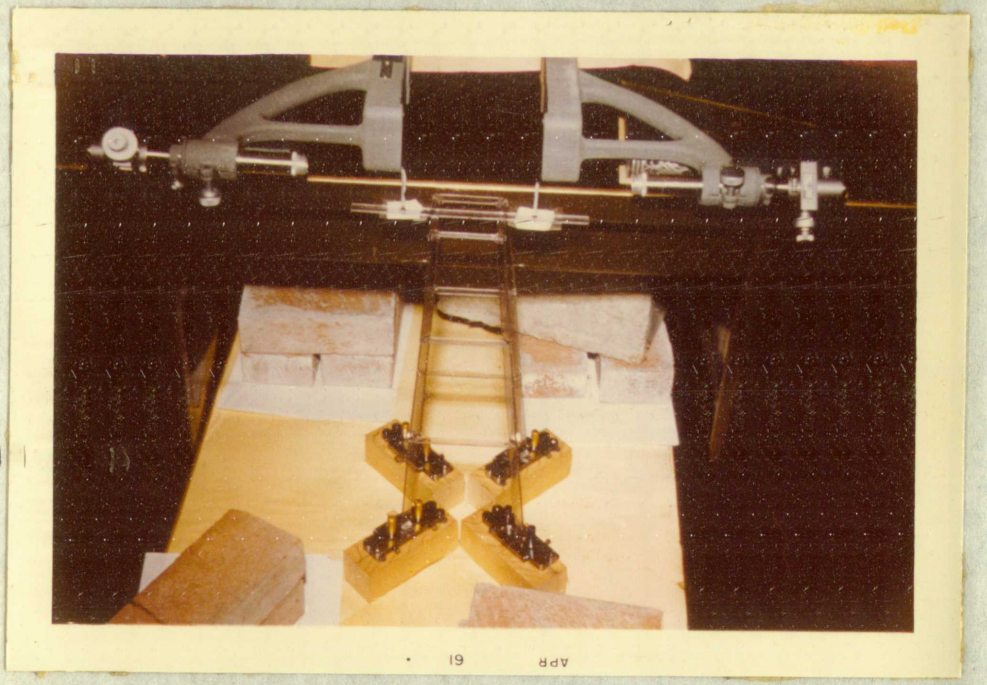

FIGURE 19

PHOTOGRAPH OF TOWER MODEL ARRANGED
FOR DISTORTIONS IN X-Z PLANE

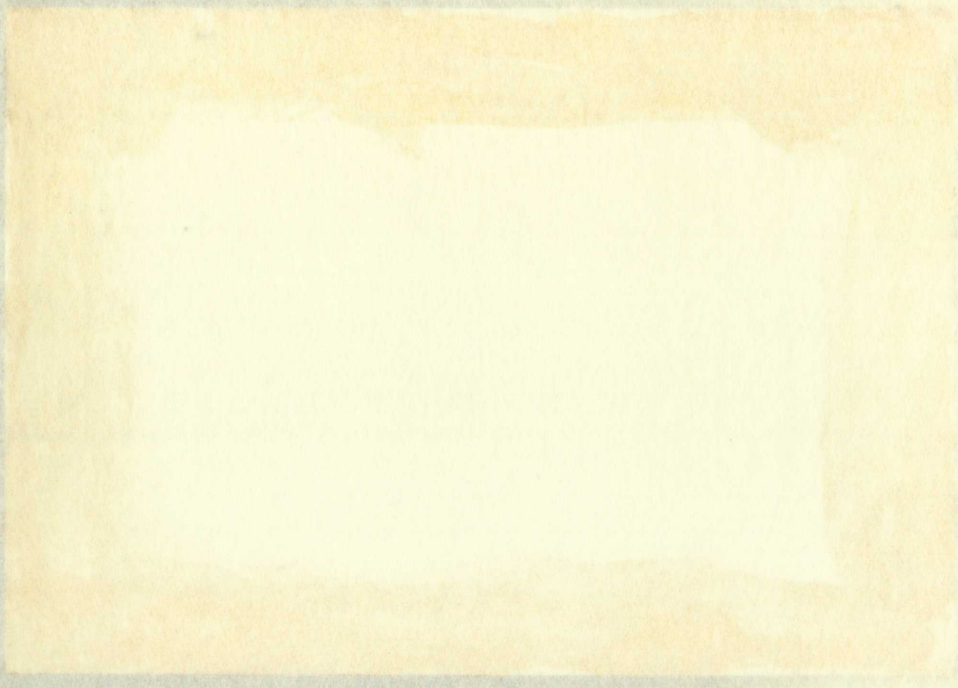

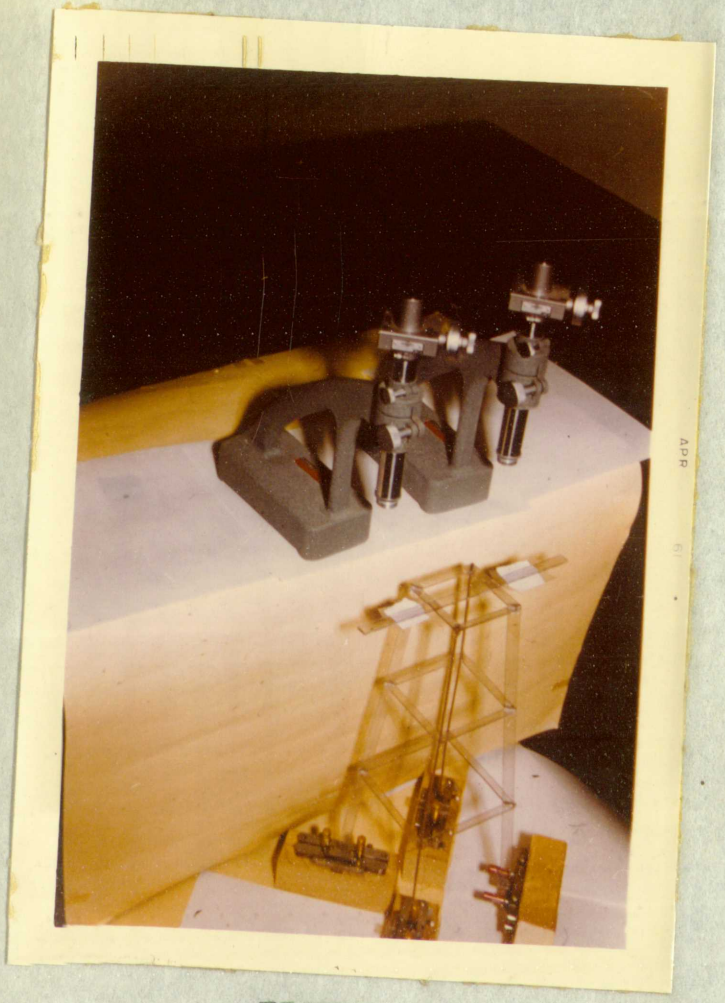

FIGURE 20

PHOTOGRAPH OF TOWER MODEL ARRANGED
FOR DISTORTIONS IN X-Y PLANE

FIGURE 20

PHOTOGRAPH OF TOWER MODEL ARRANGED
FOR DISTORTIONS IN X-Y PLANE

unit load reactions at point A caused by unit loads in the directions of the acctual loads, reactions were determined for unit loads direccted in reverse to the actual loads. Also, reactions were determined at point A for unit loads applied parallel to the transmission line at load point F. All this was necessarry to fully use the symmetric conditions of the structure.

With all the aboove unit load reactions having been determined at point A, determination of unit load reactions at the other three supports was an easy task by close observation. Appropriate unit load reactions were then multiplied by their respective load factors and combined in accordance with the principle off superposition to obtain the final results as shown in Table V below.

TABLE V

RESULTS OF TOWER PROBLEM

Component	Units	Point A	Point B	Point C	Point D
M_{xy}	kip-ft.	5.338	40.999	- 0.767	39.920
M_{xz}	kip-ft.	0.971	0.909	- 2.596	- 2.094
M_{yz}	kip-ft.	24.201	3.572	23.880	- 2.363
R_x	kips	1.597	1.581	- 0.363	1.577
R_y	kips	4.596	- 7.504	- 0.726	6.404
R_z	kips	- 0.989	- 1.413	- 0.463	0.387

Component	Units	Point A	Point B	Point C	Point D
M_{xy}	kip-in.	[illegible]	[illegible]	[illegible]	[illegible]
M_{yz}	kip-in.	[illegible]	[illegible]	[illegible]	[illegible]
M_{zx}	kip-in.	[illegible]	[illegible]	[illegible]	[illegible]
R_x	kips	[illegible]	[illegible]	[illegible]	[illegible]
R_y	kips	[illegible]	[illegible]	[illegible]	[illegible]
R_z	kips	[illegible]	[illegible]	[illegible]	[illegible]

In order to give some justification to the answers presented in Table V, a check was made by comparing the results with the conditions of static equilibrium for the entire frame treated as a free-body diagram. Such a comparison is presented in Table VI.

TABLE VI

COMPARISON OF EXPERIMENTAL RESULTS FOR THE TRANSMISSION TOWER WITH CONDITIONS OF STATIC EQUILIBRIUM

Component	Units	Experimental Reactions	External Loads	Imbalance	% Diff.
M_{xy}	kip-ft.	282.149	-282.800	- 0.651	0.23
M_{xz}	kip-ft.	- 55.976	50.000	- 5.976	11.95
M_{yz}	kip-ft.	124.543	-141.400	-16.857	11.90
R_x	kips	4.392	- 4.600	- 0.208	4.52
R_y	kips	2.770	- 3.000	- 0.230	7.67
R_z	kips	- 2.478	2.475	- 0.003	0.12

It is readily seen from Table VI that the results for the tower problem do not agree as closely with the conditions of static equilibrium as does the sign problem. There is little doubt that instability was the major contributor to these discrepencies since the variations do not form a

In order to give some justification to the theories presented in Table V, a check was made by comparing the results with the conditions of static equilibrium for the entire frame treated as a free-body diagram. Such a comparison is presented in Table VI.

TABLE VI

COMPARISON OF EXPERIMENTAL RESULTS FOR THE TRANSMISSION TOWER WITH CONDITIONS OF STATIC EQUILIBRIUM

Component	Units	Experimental Reactions	External Loads	Unbalance	% Diff.
M_{xy}	kip-ft.	282.149	-282.800	- 0.651	0.23
M_{xz}	kip-ft.	- 55.976	50.000	- 5.976	11.95
M_{yz}	kip-ft.	124.563	-141.400	-16.837	11.90
R_x	kips	4.392	- 4.600	- 0.208	4.52
R_y	kips	3.776	- 3.000	- 0.776	7.67
R_z	kips	- 2.479	2.475	- 0.004	0.12

It is readily seen from Table VI that the results for the tower problem do not agree as closely with the conditions of static equilibrium as does the sign problem. There is little doubt that instability was the major contributor to these discrepancies since the variations do not form a

particular pattern.

The maximum slenderness ratios for the columns of the tower problem were very near the same as those for the stabilized sign stanchion. However, torsion in the tower problem caused bending about the weak axes of the columns whereas torsion in the sign problem was resisted by bending of its columns about their strong axes.

During the investigation of the tower problem, it was noticed that cement creep at the joints caused considerable dispersion of readings when different time lags between inducement of deflections and taking of readings was allowed. An effort was made to overcome the effects of creep by taking readings as soon as possible after inducing the deflections. It is believed that this procedure eliminated practically all errors due to creep.

particular pattern.

The maximum slenderness ratios for the columns of the tower problem were very near the same as those for the established sign structure. However, torsion in the tower problem caused bending about the weak axes of the columns whereas torsion in the sign problem was replaced by bending of its columns about their strong axes.

During the investigation of the tower problem, it was noticed that cement creep at the joints caused considerable dispersion of readings when different time lags between inducement of deflections and taking of readings were allowed. An effort was made to overcome the effects of creep by taking readings as soon as possible after inducing the deflections. It is believed that this procedure eliminated practically all errors due to creep.

CHAPTER V

DESIGN PROPOSALS

The purpose of this chapter is to propose a redesign of the apparatus used in taking experimental data for this thesis. It has been pointed out in previous chapters that the Beggs deformeter apparatus was designed to be used in coplanar work only. Consequently, its practical application to the solution of three-dimensional problems is curtailed considerably without some changes in the present design. Such changes are discussed and illustrated in this chapter.

Gage Clamp

The experimental data for this thesis was made difficult to obtain because it was necessary to change the gage clamp mountings several times to induce the desired deflections. Figure 21 illustrates a design proposal for a universal gage to eliminate this difficulty. The parts are numbered in each figure, these numbers are used in the following discussions for identification.

The base plate and upper plate are identified by part

CHAPTER V

DESIGN PROPOSAL

The purpose of this chapter is to propose a redesign of the apparatus used in testing experimental data for this thesis. It has been pointed out in previous chapters that the Beggs deformeter apparatus was designed to be used for copilanar work only. Consequently, its practical application to the solution of three-dimensional problems is restricted considerably without some changes in the present design. Such changes are discussed and illustrated in this chapter.

Gage Clamp

The experimental data for this thesis was made difficult to obtain because it was necessary to change the gage clamp mountings several times to induce the desired deflections. Figure 21 illustrates a design proposal for a universal gage to eliminate this difficulty. The parts are numbered in each figure, these numbers are used in the following explanations for identification.

The base plate and upper plate are identical in part

numbers (1) and (2) respectively. The base plate is fastened rigidly to a drawing board (or other base) with four wood screws identified as (9). The upper plate is movable and is attached to the base plate with four cap screws and compression springs, parts (5) and (4) respectively, in a manner similar to the attachments of the two bars on the Beggs clamp. Part number (6) is an adjustable assembly used to hold the model (7). Part number (8) is a distortion plug similar to the Beggs plugs. The Beggs plugs may be used in four such locations to produce bending moments (rotations) in two different planes and translations in three mutually perpendicular directions.

In order to produce torsion in the model, four line-drilled holes are located in the four arms of the clamp and identified by part number (3). These holes must be held to a close tolerance and furnished with close tolerance pins to match. Only two such pins are used in diametrically opposite holes to produce rotation of the model support about its vertical axis while the other set of holes may be used to produce rotation of the support in the reverse

numbers (1) and (2) respectively. The base plate is fastened rigidly to a drawing board (or other base) with four wood screws identified as (9). The upper plate is movable and is attached to the base plate with four cap screws and compression springs, parts (5) and (4) respectively, in a manner similar to the attachments of the two bars on the Bedda clamp. Part number (6) is an adjustable assembly used to hold time model (7). Part number (8) is a distortion pin similar to the Bedda pins. The Bedda pins may be used in four such locations to produce bending moments (rotations) in two different planes and translations in three mutually perpendicular directions.

In order to produce torsion in the model, four line-drilled holes are located in the four arms of the clamp and identified by part number (3). These holes must be held to a close tolerance and furnished with close tolerance pins to match. Only two such pins are used in diametrically opposite holes to produce rotation of the model support about its vertical axis while the other set of holes may be used to produce rotation of the support in the reverse

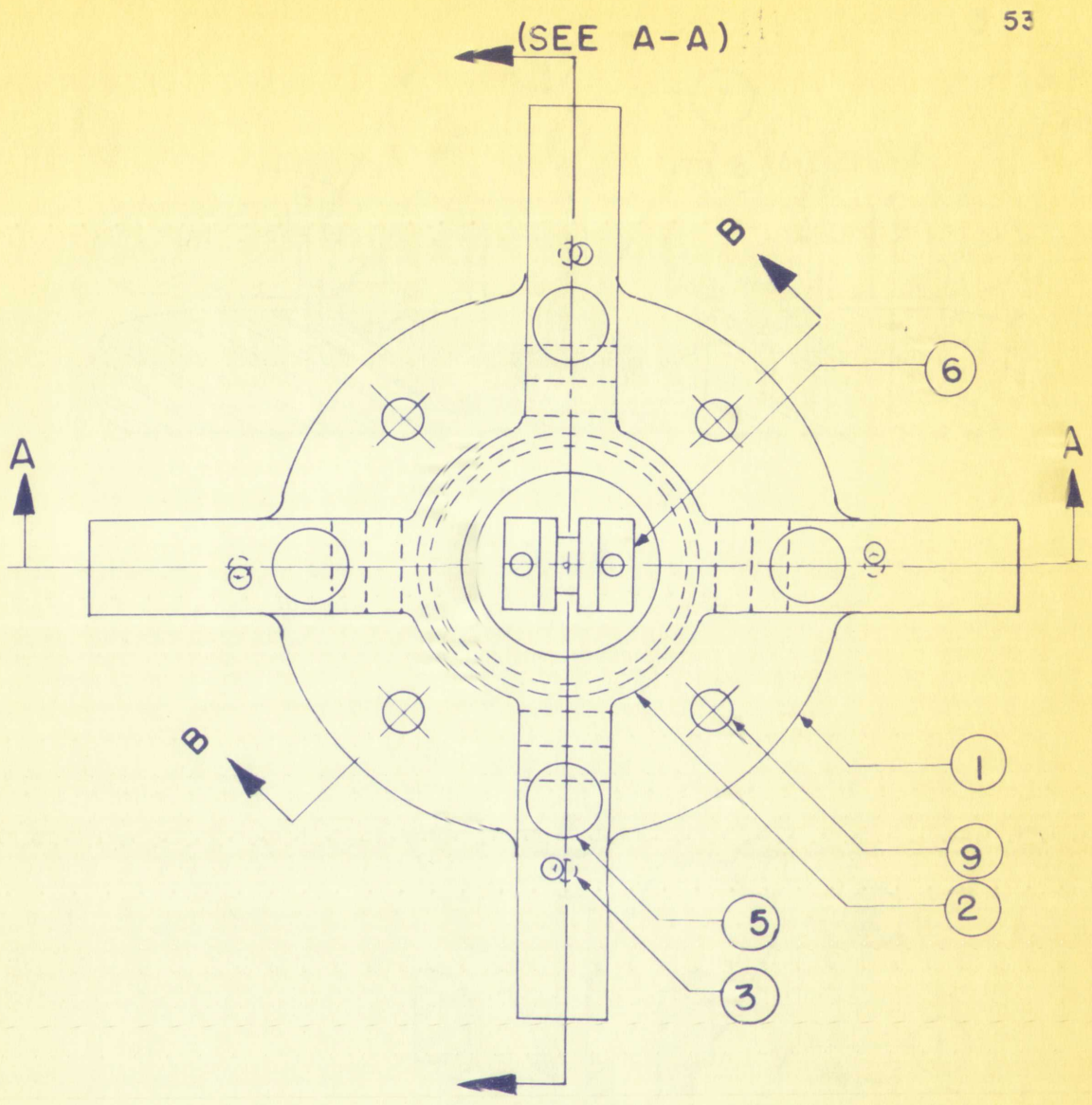

PLAN VIEW

FIGUIRE 21

UNIVERSAL GAGE CLAMP DESIGN PROPOSAL

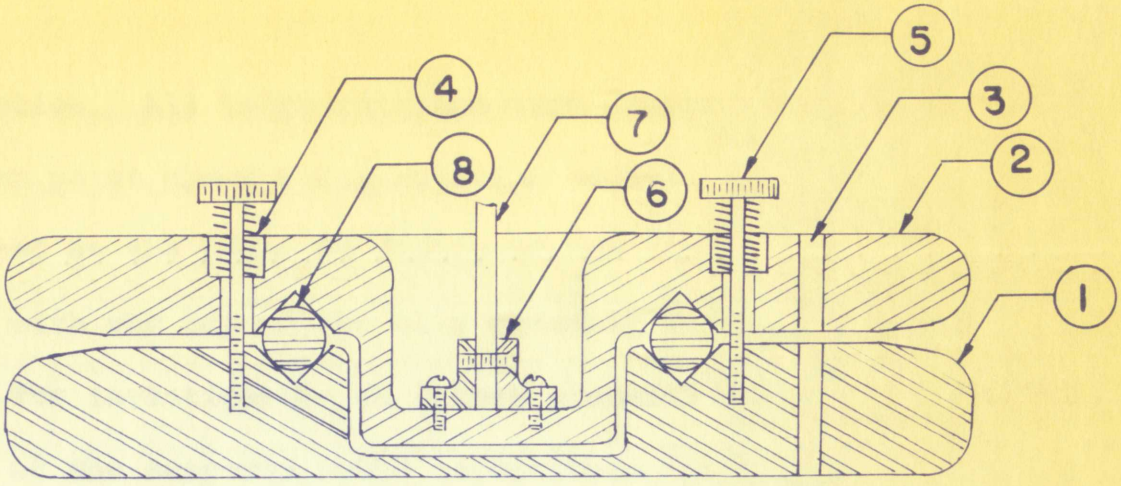

A – A

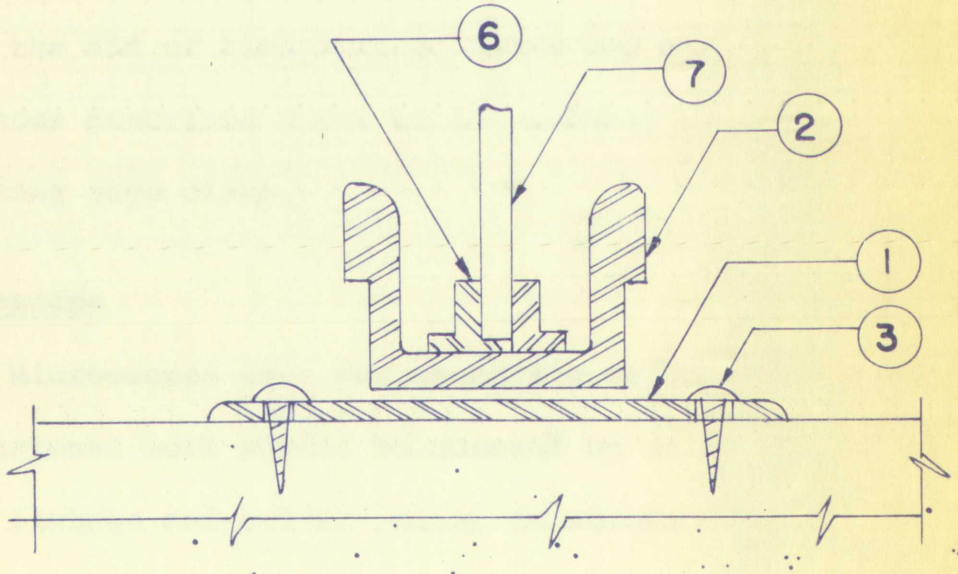

B - B

FIGURE 21 (CONTINUED)

direction. All three rotation type distortions have a common point about which rotation occurs. This point is located at the point of fixity of the support which is in line with the top of the clip assembly (6).

The investigation of stress elements in places other than at the supports would necessitate the use of a very light weight floating gage clamp similar to the present apparatus. For use in three-dimensional work, the floating gage would normally be supported entirely by the model; therefore, it is essential that the weight of the clamp be as small as possible. An adjustable sleeve arrangement with the aid of line drilled holes and matching pins similar to those described above would probably produce a better floating gage clamp.

Microscope

Microscopes used for measuring deflections in three-dimensional work should be mounted on an adjustable stand with linkage and swivel joints to accommodate easy positioning for various locations and directions of observation. Also, an adjustable focusing screw should be pro-

Microscope

Microscope used for measuring deflections in three-dimensional work should be mounted on an adjustable stand with linkage and swivel joints to accommodate easy positioning for various locations and directions of observation. Also, an adjustable focusing screw should be pro-

vided to permit focal adjustments without disturbing the position of the microscope.

CHAPTER VI

CONCLUSIONS

The solutions to example problems presented in this thesis draws one to conclude that the Beggs method can be extended to include solutions to three-dimensional problems. Such solutions may be obtained economically to a high degree of accuracy. Many problems that are practically impossible to solve mathematically may be solved mechanically with little difficulty by the Beggs method.

Incorporation of design changes to the Beggs apparatus is essential to its application to practical solutions of three-dimensional problems. Necessary changes were proposed in this thesis. Care must be exercised in model construction to eliminate creep and structural instability.

CHAPTER VI

CONCLUSIONS

The solutions to example problems presented in this thesis draws one to conclude that the Beggs method can be extended to include solutions to three-dimensional problems. Such solutions may be obtained economically to a high degree of accuracy. Many problems that are practically impossible to solve mathematically may be solved mechanically with little difficulty by the Beggs method.

Incorporation of design changes to the Beggs apparatus is essential to its application to practical solutions of three-dimensional problems. Necessary changes were proposed in this thesis. Care must be exercised in model construction to eliminate creep and structural instability.

BIBLIOGRAPHY

BIBLIOGRAPHY

BIBLIOGRAPHY

1. C. B. McCullough and E. S. Thayer, Elastic Arch Bridges, Chapter VII, John Wiley and Sons, Inc., New York, 1931.

2. J. B. Wilbur, "Structural Analysis Laboratory Research," Mass. Inst. Tech., Dept. Civil Sanitary Engr., Ser. 65, 1938, Ser. 68, 1939, Ser. 73, 1940, Ser. 80, 1941.

3. C. H. Norris, "Model Analysis of Structures," Experimental Stress Analysis, Vol. 1, No. 2, July, 1944.

4. J. B. Wilbur and C. H. Norris, "Model Analysis of Structures," Handbook of Experimental Stress Analysis, Chapter 15, John Wiley and Sons, Inc., New York, 1950.

5. G. E. Beggs, "An Accurate Mechanical Solution of Statically Indeterminate Structures by Use of Paper Models and Special Gages," ACI Proceedings, Vol. 18, pp. 58-82, 1922.

6. G. E. Beggs, "Discussion of 'Design of a Multiple Arch System'," Transactions, ASCE, Vol. 88, pp. 1208-1230, 1925.

7. G. E. Beggs, "The Use of Models in the Solution of Indeterminate Structures," J. Franklin Institute, Vol. 203, No. 3, pp. 375-386, March, 1927.

8. G. H. Lee, An Introduction to Experimental Stress Analysis, Chapter 10, John Wiley and Sons, Inc., New York, 1950.

9. J. B. Wilbur and C. H. Norris, Elementary Stress Analysis, Chapter 15, pp. 450-454, McGraw-Hill Book Company, Inc., New York, 1948.

10. J. B. Wilbur and C. H. Norris, Elementary Stress Analysis, Chapter 13, pp. 354-357, McGraw-Hill Book Company, Inc., New York, 1948.

BIBLIOGRAPHY

1. C. B. McCullough and E. B. Thayer, Plastic Arch Bridges, Chapter XII, John Wiley and Sons, Inc., New York, 1931.

2. J. B. Wilbur, "Structural Analysis Laboratory Research," Mass. Inst. Tech., Dept. Civil Sanitary Engr., Ser. 58, 1938, Ser. 68, 1939, Ser. 73, 1940, Ser. 80, 1941.

3. C. H. Norris, "Model Analysis of Structure," Experimental Stress Analysis, Vol. 1, No. 2, July, 1944.

4. J. B. Wilbur and C. H. Norris, "Model Analysis of Structures," Handbook of Experimental Stress Analysis, Chapter 15, John Wiley and Sons, Inc., New York, 1948.

5. G. E. Beggs, "An Accurate Mechanical Solution of Statically Indeterminate Structures by Use of Paper Models and Special Gages," ASCE Proceedings, Vol. 14, pp. 58-82, 1923.

6. G. E. Beggs, "Discussion of 'Design of a Multiple Arch System'," Transactions, ASCE, Vol. 89, pp. 1208-1310, 1925.

7. G. E. Beggs, "The Use of Models in the Solution of Indeterminate Structures," J. Franklin Institute, Vol. 203, No. 3, pp. 375-386, March, 1927.

8. G. H. Lee, An Introduction to Experimental Stress Analysis, Chapter 10, John Wiley and Sons, Inc., New York, 1950.

9. J. B. Wilbur and C. H. Norris, Elementary Stress Analysis, Chapter 15, pp. 450-456, McGraw-Hill Book Company, Inc., New York, 1948.

10. J. B. Wilbur and C. H. Norris, Elementary Stress Analysis, Chapter 13, pp. 354-357, McGraw-Hill Book Company, Inc., New York, 1948.

11. Dwight F. Denton, "An Evaluation of the Beggs Deformeter" (unpublished Master's thesis, The University of New Mexico, Albuquerque, 1960), pp. 16-22.

12. School of Engineering, "Notes Concerning The Beggs Deformeter Apparatus", Princeton University, New Jersey, 1954, (Mimeographed) pp. 1-3.

13. "A Manual for Architects, Engineers and Fabricators of Buildings and Other Steel Structures" American Institute of Steel Construction, New York, 1955.

1.1.. Dwight P. Denton, "An Evaluation of the Zeroppa Deflectometer" (unpublished Master's thesis, The University of New Mexico, Albuquerque, 1960), pp. 16-22.

1.2.. School of Engineering, "Notes Concerning the Deflectometer Apparatus", Princeton University, Princeton, New Jersey, 1954, (Mimeographed) pp. 1-3.

1.3.. "A Manual for Architects, Engineers and Fabricators of Buildings and other Steel Structures" American Institute of Steel Construction, New York, 1963.

APPENDIX A

APPENDIX A

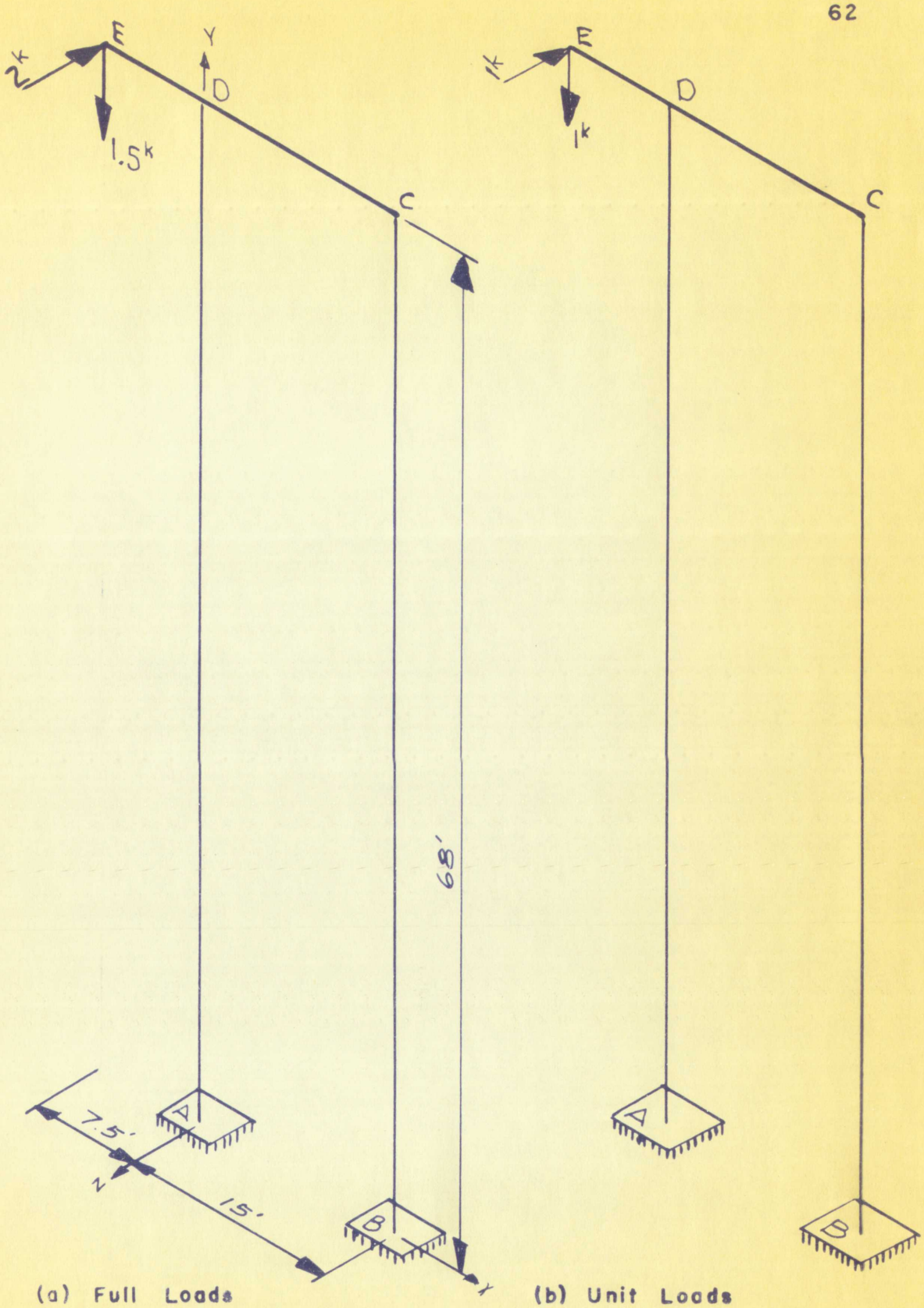

FIGURE 8

LOADING CONDITIONS AND DIMENSIONS OF UNSTABLE SIGN STANCHION

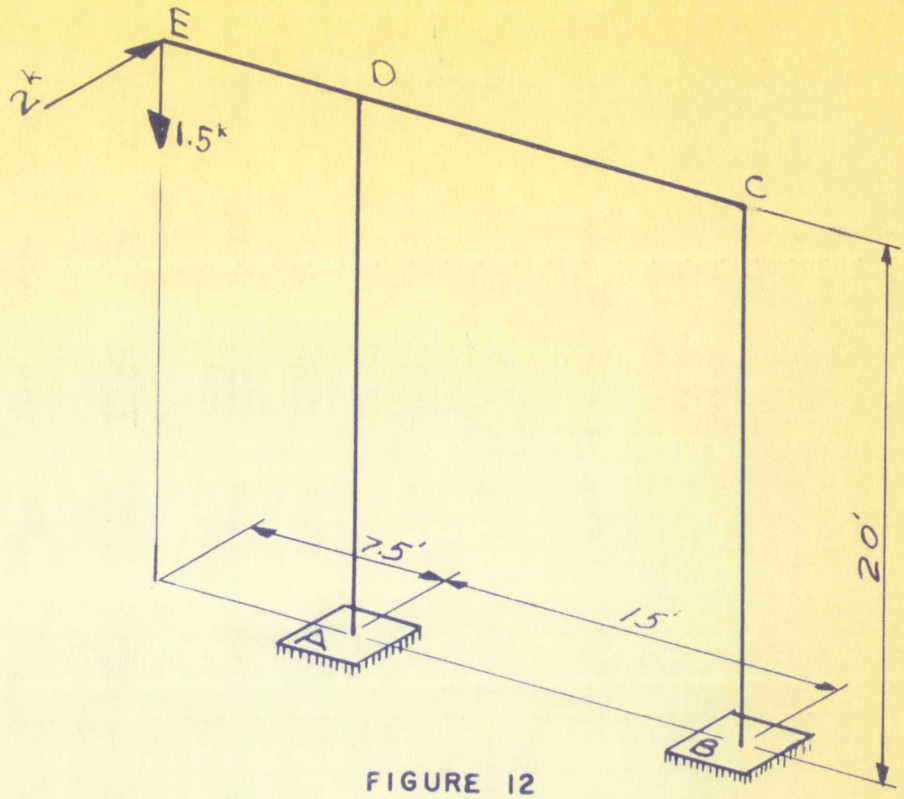

FIGURE 12

LOADING CONDITIONS AND DIMENSIONS OF STABLE SIGN STANCHION

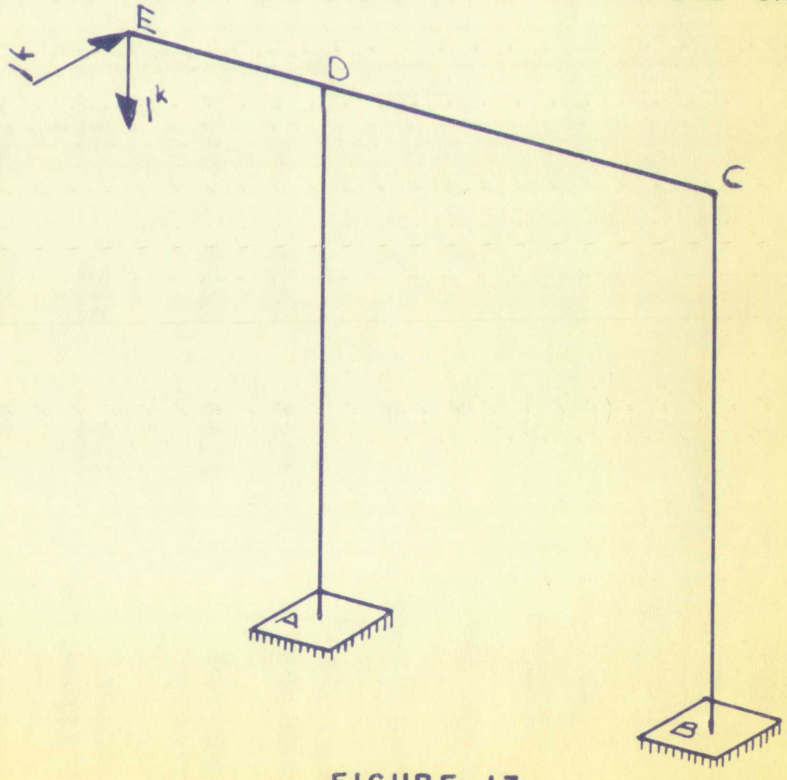

FIGURE 13

UNIT LOADING CONDITIONS OF STABLE SIGN STANCHION

TABLE VII

EXPERIMENTAL SOLUTION TO UNSTABLE SIGN PROBLEM, VERTICAL LOADS ONLY

Component	M_{Axz}	M_{Bxz}	M_{Ayz}	M_{Byz}	R_{Ax}	R_{Bx}	R_{Ay}	R_{By}	R_{Az}	R_{Bz}
Calibration Factor	$\frac{1}{256}$	$\frac{1}{256}$	$\frac{1}{256}$	$\frac{1}{256}$	$\frac{1}{1285}$	$\frac{1}{1285}$	$\frac{1}{1285}$	$\frac{1}{1285}$	$\frac{1}{1287}$	$\frac{1}{1287}$
Direct Reading	1979	1976	2642	2572	1640	1892	3028	2512	1958	531
Reversed Reading	1979	1975	2639	2570	1632	1903	1092	3163	1965	526
Difference	0	1	3	2	8	11	1936	651	7	5
Scale Factor	4	4	4	4	1	1	1	1	1	1
Unit Load Reactions	0	-0.016	0.047	0.031	-0.006	-0.008	1.507	-0.507	-0.005	0.004
Load Factor	1.5	1.5	1.5	1.5	1.5	1.5	1.5	1.5	1.5	1.5
Reactions	0	-0.024	0.070	0.046	-0.009	-0.012	2.260	-0.760	-0.007	0.006
Units	kip-ft	kip-ft	kip-ft	kip-ft	kips	kips	kips	kips	kips	kips

PART VII

EXPERIMENTAL SOLUTION OF MOTION DUE TO IMPULSIVE AND PERIODIC FORCES ONLY

TABLE VIII

EXPERIMENTAL SOLUTION TO UNSTABLE SIGN PROBLEM, HORIZONTAL LOADS ONLY

Component	M_{Axz}	M_{Bxz}	M_{Ayz}	M_{Byz}	R_{Ax}	R_{Bx}	R_{Ay}	R_{By}	R_{Az}	R_{Bz}
Calibration Factor	$\frac{1}{256}$	$\frac{1}{256}$	$\frac{1}{256}$	$\frac{1}{256}$	$\frac{1}{1285}$	$\frac{1}{1285}$	$\frac{1}{1285}$	$\frac{1}{1285}$	$\frac{1}{1287}$	$\frac{1}{1287}$
Direct Reading	1853	1584	- 128	383	1503	1467	134	1298	638	1070
Reversed Reading	1498	1836	3808	2233	1503	1467	133	1296	352	1289
Difference	355	252	3937	1850	0	0	1	2	286	219
Scale Factor	4	4	4	4	1	1	1	1	1	1
Unit Load Reactions	- 5.550	-3.940	- 61.500	28.900	0	0	0.001	0.002	0.153	-0.170
Load Factor	2	2	2	2	2	2	2	2	2	2
Reactions	-11.100	-7.880	-123.000	57.800	0	0	0.002	0.004	0.306	-0.340
Units	kip-ft	kip-ft	kip-ft	kip-ft	kips	kips	kips	kips	kips	kips

TABLE XVIII

EXPERIMENTAL SOLUTION TO DISTURBED MOTION, MEDIUM ALTITUDE, NORMAL LOADS ONLY

Component	$M_{\dot{w}}$	$M_{w\|w\|}$	M_{qS}	M_{w}	M_{q}	$Z_{\dot{w}}$	$Z_{w\|w\|}$	Z_{qS}	Z_{w}	Z_{q}	$X_{\dot{u}}$	$X_{u\|u\|}$	X_{rr}	X_{u}	X_{r}
	$\frac{1}{ft}$	$\frac{1}{ft}$	$\frac{1}{ft}$	$\frac{1}{sec}$	$\frac{1}{sec}$	$\frac{1}{ft}$	$\frac{1}{ft}$	$\frac{1}{ft}$	$\frac{1}{sec}$	$\frac{1}{sec}$	$\frac{1}{ft}$	$\frac{1}{ft}$	$\frac{1}{ft}$	$\frac{1}{sec}$	$\frac{1}{sec}$
Stability Derivatives	.0170	.0138	.038	1.208	1.147	.1203	.1582	.325	1.325	1.147	.1203	.1582	.325	1.325	1.147
Direct Reversed	.0170	.0138	.038	1.208	1.147	.1203	.1582	.325	1.325	1.147	.1203	.1582	.325	1.325	1.147
Control Derivatives	.515	.1581	.325	1.325	0	0	.1820	.3231	.325	.325	1.284	- 1.58	.3808	1.832	1.4708
Elevator	1	1	1	1	1	1	1	1	1	1	1	1	1	1	1
Aileron	1	1	1	1	1	1	1	1	1	1	1	1	1	1	1
Rudder	1	1	1	1	1	1	1	1	1	1	1	1	1	1	1
Unit Loads															
Aerodynamic	-0.1230	0.1223	0.005	0.001	0	0	$-2.38.005$	-21.200	-3.220	-3.220					
Body Axis	S	S	S	S	S	S	S	S	S	S					
Resultant	$-0.3\#0$	$0.30\#$	$0.00\#$	$0.00\#$	0	0	$\#50.0$	$\#1.800$	$-1\#3\#.000$	-11.100					
Gravity															

TABLE IX

EXPERIMENTAL SOLUTION TO UNSTABLE SIGN PROBLEM, COMBINED LOADING

Component	M_{Axz}	M_{Bxz}	M_{Ayz}	M_{Byz}	R_{Ax}	R_{Bx}	R_{Ay}	R_{By}	R_{Az}	R_{Bz}
Reactions Due to Vertical Loads	0	-0.024	0.070	0.046	-0.009	-0.012	2.260	-0.760	-0.007	0.006
Reactions Due to Horizontal Loads	-11.100	-7.880	-123.000	57.800	0	0	0.002	0.004	0.306	-0.340
Combined Results	-11.100	-7.904	-122.030	57.846	-0.009	-0.012	2.262	-0.756	0.299	-0.334
Units	kip-ft	kip-ft	kip-ft	kip-ft	kips	kips	kips	kips	kips	kips

TABLE IX

EXPERIMENTAL SOLUTION TO UNSTABLE BEAM PROBLEM, CONCENTRATED LOADING

Component	M_{xx}	M_{yy}	M_{xy}	P_{xx}	P_{xy}	P_{yy}	P_{zz}
Beam Loads Due to Vertical Loads	0	-0.054	0.070	-0.046	-0.012	2.250	-0.750	-0.007	0.006
Reactions Due to Horizontal Loads	-11.100	-7.880	-123.000	57.800	0	0.002	0.906	0.306	-0.730
Combined Results	-11.100	-7.934	-123.030	57.846	-0.059	-0.010	2.252	0.299	-0.736
Units	Kip-ft	Kip-ft	Kip-ft	Kips	Kips	Kips	Kips	Kips	Kips

TABLE X

EXPERIMENTAL SOLUTION TO STABLE SIGN PROBLEM, VERTICAL LOADS ONLY

Component	M_{Axz}	M_{Bxz}	M_{Ayz}	M_{Byz}	R_{Ax}	R_{Bx}	R_{Ay}	R_{By}	R_{Az}	R_{Bz}
Calibration Factor	$\frac{1}{256}$	$\frac{1}{256}$	$\frac{1}{256}$	$\frac{1}{256}$	$\frac{1}{1285}$	$\frac{1}{1285}$	$\frac{1}{1285}$	$\frac{1}{1285}$	$\frac{1}{1287}$	$\frac{1}{1287}$
Direct Reading	2516	2538	1658	1621	2279	2676	2712	1483	1738	1650
Reversed Reading	2519	2538	1657	1621	2276	2672	775	2126	1744	1650
Difference	3	0	1	0	3	4	1937	643	6	0
Scale Factor	4	4	4	4	1	1	1	1	1	1
Unit Load Reaction	0.047	0	-0.016	0	0.002	0.004	1.505	-0.501	-0.005	0
Load Factor	1.5	1.5	1.5	1.5	1.5	1.5	1.5	1.5	1.5	1.5
Reactions	0.070	0	-0.024	0	0.003	0.006	2.260	-0.751	-0.007	0
Units	kip-ft	kip-ft	kip-ft	kip-ft	kips	kips	kips	kips	kips	kips

TABLE X

EXPERIMENTAL SOLUTION TO STRAIN RATE PROBLEM, ASSUMING TWO COMPONENTS

Components	M^{xx}	M^{yy}	M^{zz}	M^{xy}	M^{yz}	M^{zx}	K^{xx}	K^{yy}	K^{zz}	K^{xy}	K^{yz}	K^{zx}
Calibration Factor	$\frac{1}{.520}$	$\frac{1}{.520}$	$\frac{1}{.520}$	$\frac{1}{.520}$	$\frac{1}{.520}$	$\frac{1}{.520}$	$\frac{1}{.1582}$	$\frac{1}{.1582}$	$\frac{1}{.1582}$	$\frac{1}{.1582}$	$\frac{1}{.1582}$	$\frac{1}{.1582}$
Direct Reading	.5210	.5238	.5238	.1581	.1581	.1581	.5219	.5273	.1581	.1581	.1581	.1581
Observed Result	.5250	.5250	.5250	.1581	.1581	.1581	.5250	.5250	.1581	.1581	.1581	.1581
Differences	0	0	0	0	0	0	3	4	.0031	0	0	0
Scale Factor	1	1	1	1	1	1	1	1	1	1	1	1
Unit Load Reaction	0	0	0	0	0	0	.0016	.0047	.0047	.0004	0	0
Load Factor	1.5	1.5	1.5	1.5	1.5	1.5	1.5	1.5	1.5	1.5	1.5	1.5
Resultant	0	0	0	0	0	0	.0024	.0070	.0070	.0006	0	0

TABLE XI

EXPERIMENTAL SOLUTION TO STABLE SIGN PROBLEM, HORIZONTAL LOADS ONLY

Component	M_{Axz}	M_{Bxz}	M_{Ayz}	M_{Byz}	R_{Ax}	R_{Bx}	R_{Ay}	R_{By}	R_{Az}	R_{Bz}
Calibration Factor	$\frac{1}{256}$	$\frac{1}{256}$	$\frac{1}{256}$	$\frac{1}{256}$	$\frac{1}{1285}$	$\frac{1}{1285}$	$\frac{1}{1285}$	$\frac{1}{1285}$	$\frac{1}{1287}$	$\frac{1}{1287}$
Direct Reading	2040	2060	3075	1237	694	3044	1918	1713	2781	2120
Reversed Reading	1917	1960	1500	1527	682	3034	1926	1713	1146	1771
Difference	123	100	1575	290	12	10	8	0	1635	349
Scale Factor	4	4	4	4	1	1	1	1	1	1
Unit Load Reaction	-1.923	-1.561	-24.650	4.540	0.009	-0.008	-0.006	0	1.272	-0.271
Load Factor	2	2	2	2	2	2	2	2	2	2
Reactions	-3.846	-3.122	-49.300	9.080	0.018	-0.016	-0.012	0	2.544	-0.542
Units	kip-ft	kip-ft	kip-ft	kip-ft	kips	kips	kips	kips	kips	kips

TABLE XI

EXPERIMENTAL EVALUATION OF SIMPLE BIAS ESTIMATION, MULTIPROCESSOR HORIZONTAL LOADS ONLY

Component	M_{BAS}	R_{BAS}	R_{VA}	R_{MA}	$\frac{I_{SB2}}{I_{SB1}}$	$\frac{I_{SB2}}{I_{SB1}}$	$\frac{I_{SB1}}{I_{SB1}}$	M_{PAS}	M_{PAS}	$\frac{I_{SB2}}{I_{SB1}}$	$\frac{I_{SB2}}{I_{SB1}}$	$\frac{I_{SB1}}{I_{SB1}}$	M_{PAS}	M_{PAS}	$\frac{I_{SB2}}{I_{SB1}}$	$\frac{I_{SB2}}{I_{SB1}}$	$\frac{I_{SB1}}{I_{SB1}}$	Units
Restraint Restrained	1871	7800	7200	7251	685	3034	7858	7373	7748	1	1	1	0	0	0.0000	-0.008	0.0018	Unit load factor
Restraint Direct	5040	5020	3012	7531	444	3044	7818	7373	5187	1	1	1	0	0	0.0000	-0.008	0.0018	Restraint reaction
Active Configuration	$\frac{I_{SB1}}{I}$	$\frac{I_{SB1}}{I}$	$\frac{I_{SB1}}{I}$	$\frac{I_{SB1}}{I}$	M_{PAS}	M_{PAS}	$\frac{I_{SB1}}{I}$	$\frac{I_{SB2}}{I}$	$\frac{I_{SB2}}{I}$	$\frac{I_{SB2}}{I}$	$\frac{I_{SB1}}{I}$	$\frac{I_{SB1}}{I}$	M_{PAS}	M_{PAS}	$\frac{I_{SB1}}{I}$	$\frac{I_{SB1}}{I}$	$\frac{I_{SB1}}{I}$	Component
Active factor	4	4	4	4	1	1	1	1	1	1	1	1	1	1	1	1	1	Active factor
Difference	153	100	1212	320	15	10	8	0	1032	340	1	1	1	0	1.2512	-0.517	-0.2545	Difference
Restrained Restrained	1871	7800	7200	7251	685	3034	7858	7373	7748	7737	1	1	1	0	1.2512	-0.517	-0.2545	Restrained Restrained
Restraint Direct	5040	5020	3012	7531	444	3044	7818	7373	5187	5150	1	1	1	0	1.2512	-0.517	-0.2545	Restraint Direct
Unit load factor	-1.2512	-1.2512	-5.4520	4.2540	0.0000	0.0000	-0.008	0.0018	-0.2545	-0.517	1.2512	0.0000	0.0000	0.0000	0.0000	0.0000	0.0000	Restrained load factor
Restrained reaction	-3.8840	-3.1552	-4.5300	3.080	0.0018	-0.0018	-0.0018	-0.2545	-0.2545	-0.2545	0.0000	0.0000	0.0000	0.0000	0.0000	0.0000	0.0000	Unrestrained reaction

TABLE XII

EXPERIMENTAL SOLUTION TO STABLE SIGN PROBLEM, COMBINED LOADING

Component	M_{Axz}	M_{Bxz}	M_{Ayz}	M_{Byz}	R_{Ax}	R_{Bx}	R_{Ay}	R_{By}	R_{Az}	R_{Bz}
Reactions Due to Vertical Loads	0.070	0	- 0.024	0	0.003	0.006	2.260	-0.571	-0.007	0
Reactions Due to Horizontal Loads	-3.846	-3.122	-49.300	9.080	0.018	-0.016	-0.012	0	2.544	-0.542
Combined Results	-3.776	-3.122	-49.324	9.080	0.021	-0.010	2.248	-0.571	2.537	-0.542
Units	kip-ft	kip-ft	kip-ft	kip-ft	kips	kips	kips	kips	kips	kips

TABLE XIII

DISPLACEMENT, ROTATION AND STRESS RESULTANTS, CONCENTRATED LOADING

Component	M_x^A	M_x^B	M_y^A	M_y^B	V_x^A	V_x^B	V_y^A	V_y^B	R_A	R_B
Reactions Due to Vertical Loads	0.070	0	0.054	0	0.003	0.000	2.260	-0.271	-0.007	0
Reactions Due to Horizontal Loads	-3.846	-3.125	-99.300	99.080	0.078	-0.078	0	2.544	-0.542	
Combined Reactions	-3.776	-3.253	-99.354	99.080	0.081	0.000	2.260	-0.271	2.537	-0.542
Units	kip-ft	kip-ft	kip-ft	kip-ft	kips	kips	kips	kips	kips	kips

SIMPLIFIED MATHEMATICAL ANALYSIS OF SIGN PROBLEMS

Vertical Load Only

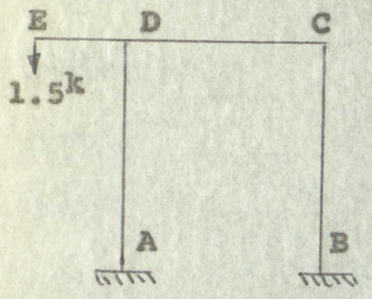

SKETCH

Properties:

I_{z-z} of CDE = 1.636×10^6 in.^{4}

I_{y-y} of CDE = 3.73×10^5 in.^{4}

I_{z-z} of AD & BC = 148 in.^{4}

I_{x-x} of AD & BC = 4840 in.^{4}

Since member CDE is very stiff in comparison to AD and BC, it is assumed that CDE acts as a simply supported beam with supports at D and C. This assumption makes a statically determinate problem of the structure. When a summation of moments is taken with respect to the z-axis of each support A and B, then R_{By} and R_{Ay} are respectively -0.750 kips and 2.250 kips. It is assumed that no reactions occur in the y-z plane.

It becomes apparent by closely observing the properties listed above and the dimensions of the structure that bending

SIMPLIFIED MATHEMATICAL ANALYSIS OF RIGID FRAMES

Vertical Load Only

SKETCH

Properties:

I_{x-x} of AD & BC = 6840 in.^{4}

I_{z-z} of AD & BC = 148 in.^{4}

I_{y-y} of CDE = $3.73x10^3$ in.^{4}

I_{z-z} of CDE = $1.636x10^3$ in.^{4}

Since member CDE is very stiff in comparison to AD and BC, it is assumed that CDE acts as a simply supported beam with supports at D and C. This assumption makes a statically determinate problem of the structure. When a summation of moments is taken with respect to the z-axis of each support A and B, then R_{By} and R_{Ay} are respectively -0.750 kips and 2.250 kips. It is assumed that no reactions occur in the y-z plane.

It becomes apparent by closely observing the properties listed above and the dimensions of the structure that bending

moments in the x-y plane at points C and D are almost entirely resisted by the horizontal member CDE due to its greater stiffness. Furthermore, distribution factors, as computed for the moment distribution method of analysis indicate that a negligible portion of the fixed-end moments are distributed to the vertical members at joints C and D. The distribution factors in question are 0.9999321 for the horizontal member and 0.0000679 for the vertical members at joints C and D. When sideway of the structure is considered, it is apparent that both vertical members equally share any reactions in the x-y plane; hence, this leads one to conclude that no horizontal reactions occur in the x-direction at points A and B since such reactions for sideway alone must be equal in magnitude and direction, therefore, requiring an imbalance of horizontal forces at A and B due to the loads alone which was shown to be negligible.

moments in the x-y plane at points C and D are almost entirely resisted by the horizontal member CD, due to its greater stiffness. Furthermore, distribution factors, as computed for the moment distribution method of analysis, indicate that a negligible portion of the fixed-end moments are distributed to the vertical members at joints C and D. The distribution factors in question are 0.999923 for the horizontal member and 0.000079 for the vertical members at joints C and D. When midway of the structure is considered, it is apparent that both vertical members equally share any reactions in the x-y plane; hence, this leads one to conclude that no horizontal reactions occur in the x-direction at points A and B since such reactions for sidesway alone must be equal in magnitude and direction, therefore, requiring an imbalance of horizontal forces at A and B due to the loads alone which was shown to be negligible.

Horizontal Load Only

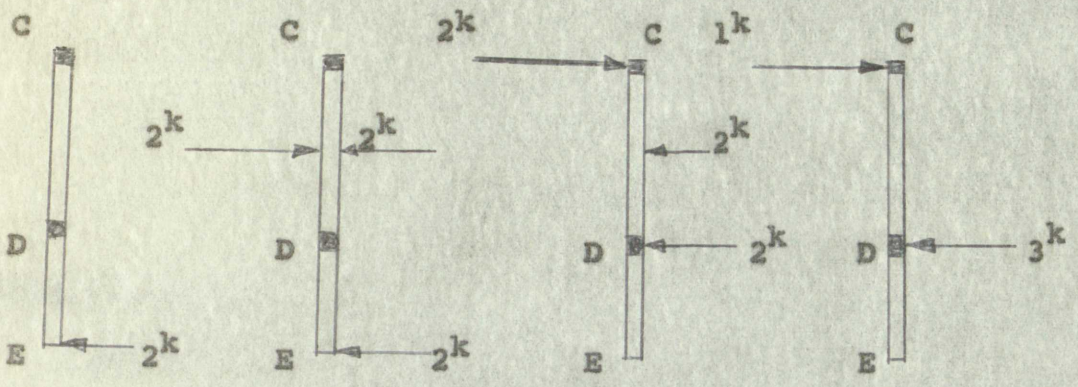

SKETCH

Assume CDE is rigid, then the problem may be solved diagramatically as shown in the sketch to determine the loads transmitted to the tops of the columns at C and D by the rigid beam CDE. Then, by applying the equations of statics to the columns, the following results are easily obtained.

Unstable Frame:

M_{Ayz} = -204 kip-ft

M_{Byz} = 68 kip-ft

R_{Az} = 3 kips

R_{Bz} = - 1 kip

Horizontal Load Only

SKETCH

Assume CDE is rigid, then the problem may be solved diagramatically as shown in the sketch to determine the loads transmitted to the tops of the columns at C and D by the rigid beam CDE. Then, by applying the equations of statics to the column, the following results are easily obtained.

Unstable Frame:

R_{Bx} = - 1 kip

R_{Ax} = 3 kips

M_{Bx} = 68 kip-ft

M_{Ax} = -204 kip-ft

Stable Frame: $M_{Ayz} = 60$ kip-ft

$M_{Byz} = 20$ kip-ft

$R_{Az} = 3$ kips

$R_{Bz} = 1$ kip

Combined Loads

The results of the combined loads are shown in Table XIII for both the unstable and stable sign problems.

TABLE XIII

MATHEMATICAL RESULTS FOR BOTH SIGN PROBLEMS

Component	Units	Unstable Sign	Stable Sign
M_{Ayz}	kip-ft.	- 204.000	- 60.000
M_{Byz}	kip-ft.	68.000	20.000
R_{Ay}	kips	2.250	2.250
R_{By}	kips	- 0.750	- 0.750
R_{Az}	kips	3.000	3.000
R_{Bz}	kips	- 1.000	- 1.000

Stable frame:

M_{Ax} = 60 kip-ft

M_{Bx} = 20 kip-ft

R_{Ax} = 3 kips

R_{Bx} = 1 kip

Combined Loads

The results of the combined loads are shown in Table XIII for both the unstable and stable sign problems.

TABLE XIII

MATHEMATICAL RESULTS FOR BOTH SIGN PROBLEMS

Component	Units	Unstable Sign	Stable Sign
M_{Ax}	kip-ft.	- 204.000	- 60.000
M_{Bx}	kip-ft.	68.000	20.000
R_{Ay}	kips	2.250	2.250
R_{By}	kips	- 0.750	- 0.750
R_{Ax}	kips	3.000	3.000
R_{Bx}	kips	- 1.000	- 1.000

APPENDIX B

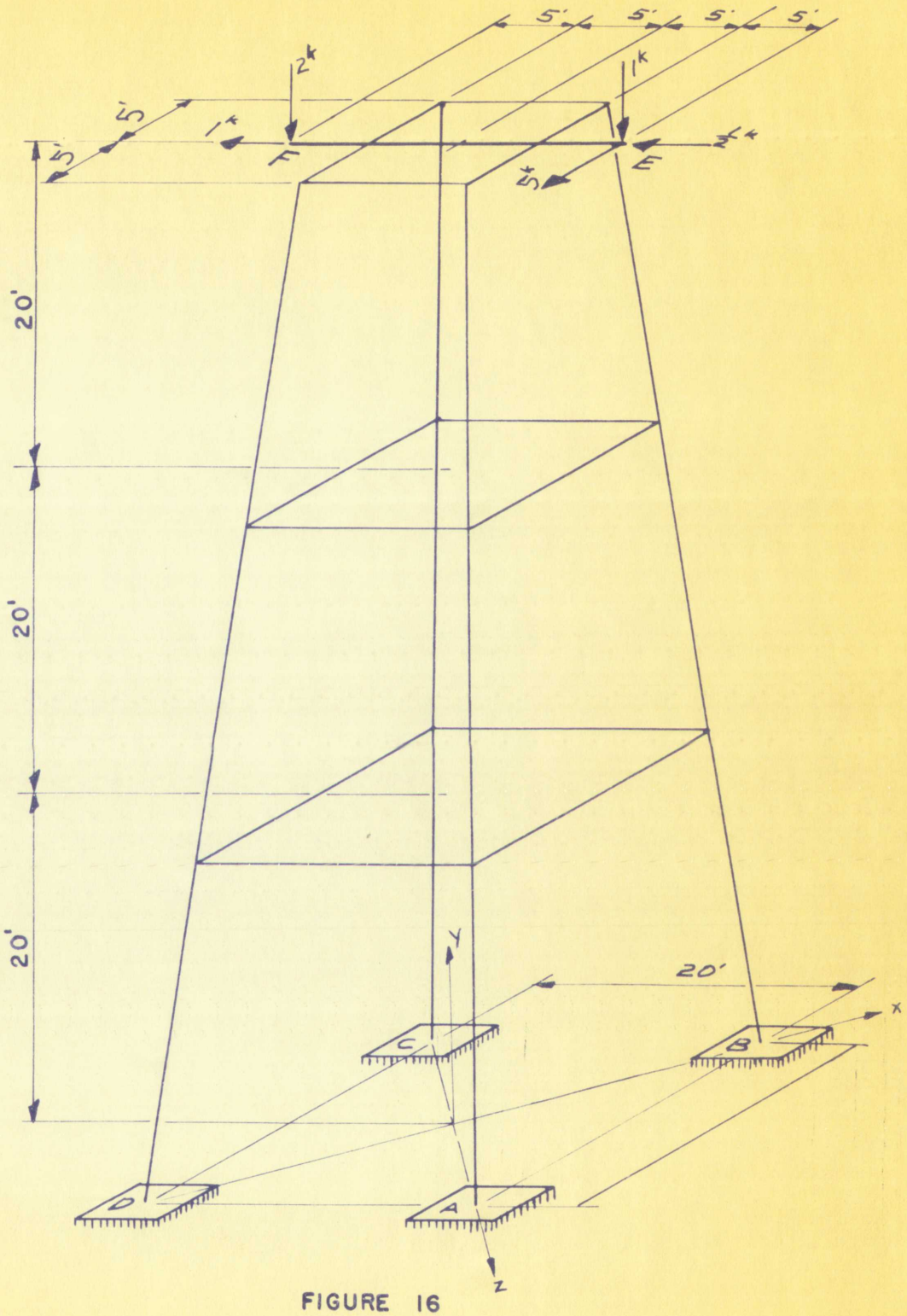

FIGURE 16

LOADING CONDITIONS AND DIMENSIONS OF TOWER STRUCTURE

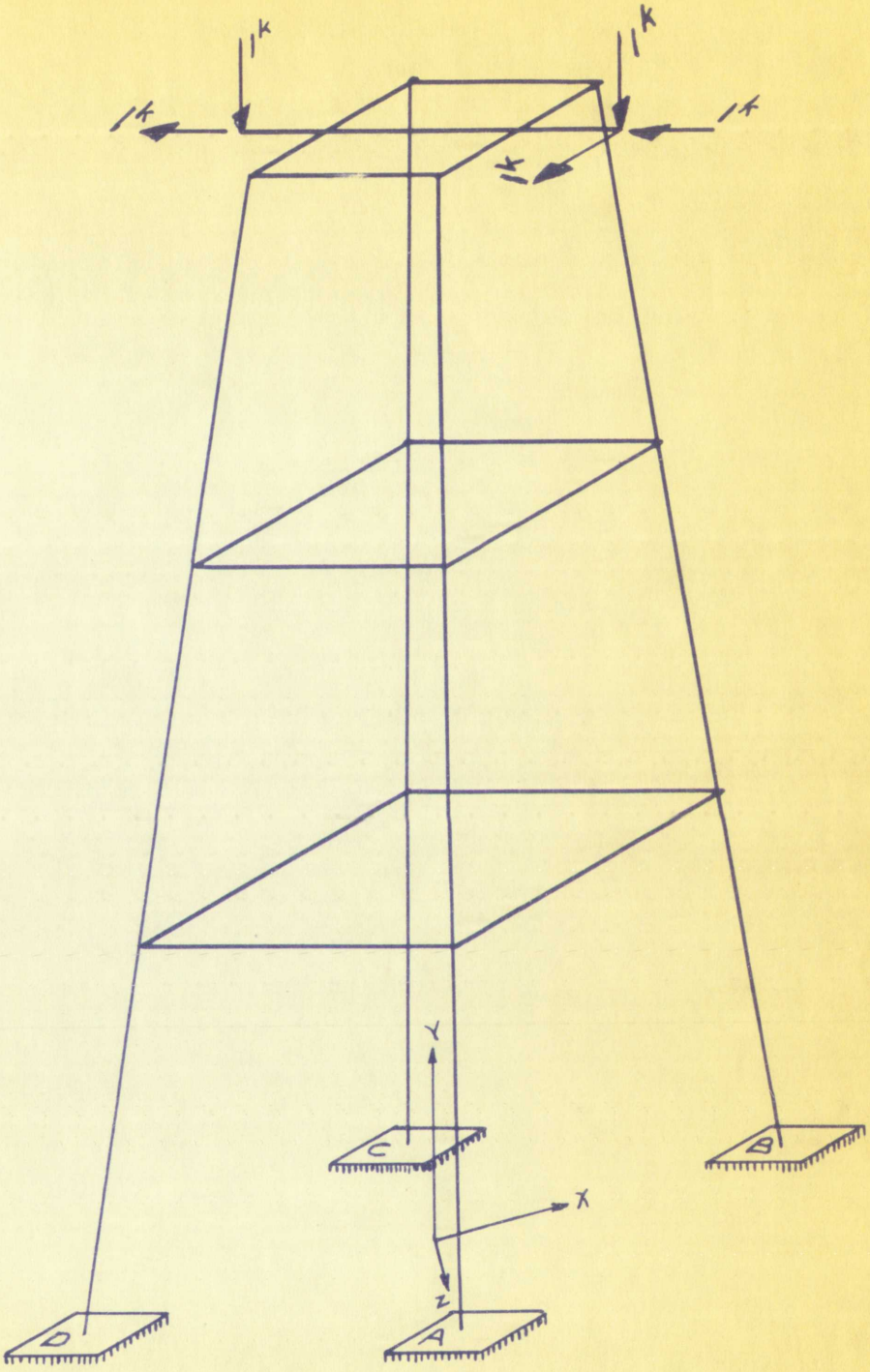

FIGURE 22

UNIT LOADING CONDITIONS OF TOWER STRUCTURE

TABLE XIV

COMPUTATION OF REACTIONS DUE TO A UNIT LOAD AT E PARALLEL TO BA IN A DIRECTION FROM B TOWARD A

Component	M_{Axy}	M_{Axz}	M_{Ayz}	R_{Ax}	R_{Ay}	R_{Az}
Calibration Factor	$\frac{1}{256}$	$\frac{1}{256}$	$\frac{1}{256}$	$\frac{1}{1285}$	$\frac{1}{1285}$	$\frac{1}{1289}$
Direct Reading	2679	1506	896	1240	1803	2431
Reversed Reading	2622	1494	1313	1627	3358	2100
Difference	57	12	417	387	1555	331
Scale Factor	4	4	4	1	1	1
Unit Load Reactions	0.891	0.188	6.520	0.301	1.210	-0.257
Reactions Due to Reversed Loading	-0.891	-0.188	-6.520	-0.301	-1.210	0.257
Units	kip-ft	kip-ft	kip-ft	kips	kips	kips

TABLE XIV

CONTRIBUTION OF REACTIONS DUE TO A UNIT LOAD AT
B TRAVELING TO B IN A BRIDGE MOMENTS FROM B TOWARD A

Components	M_{AY}	M_{AX}	M_{BX}	R_{AY}	R_{AX}
Gallbladder	$\frac{1}{256}$	$\frac{256}{1}$	$\frac{1}{1296}$	$\frac{1}{1296}$	$\frac{1}{1296}$
Bladder	2079	1296	256	1296	1296
Spleen	1296	1296	1296	1296	1296
Pancreas	1296	1296	1296	1296	1296
Duodenum	1296	1296	1296	1296	1296
Jejunum	1296	1296	1296	1296	1296
Ileum	1296	1296	1296	1296	1296
Appendix	1296	1296	1296	1296	1296
Ascending Colon	1296	1296	1296	1296	1296
Transverse Colon	1296	1296	1296	1296	1296
Descending Colon	1296	1296	1296	1296	1296
Sigmoid	1296	1296	1296	1296	1296
Rectum	1296	1296	1296	1296	1296
Upper Large Intestine	1296	1296	1296	1296	1296
Lower Large Intestine	1296	1296	1296	1296	1296
Small Intestine	1296	1296	1296	1296	1296
Stomach	1296	1296	1296	1296	1296
Esophagus	1296	1296	1296	1296	1296
Liver	1296	1296	1296	1296	1296
Kidneys	1296	1296	1296	1296	1296
Urinary Bladder	1296	1296	1296	1296	1296
Testes	1296	1296	1296	1296	1296
Uterus	1296	1296	1296	1296	1296
Ovaries	1296	1296	1296	1296	1296
Breasts	1296	1296	1296	1296	1296
Bone Marrow	1296	1296	1296	1296	1296
Skin	1296	1296	1296	1296	1296
Remainder	1296	1296	1296	1296	1296

TABLE XV

COMPUTATION OF REACTIONS DUE TO A UNIT LOAD AT E PARALLEL TO EF IN A DIRECTION FROM E TOWARD F

Component	M_{Axy}	M_{Axz}	M_{Ayz}	R_{Ax}	R_{Ay}	R_{Az}
Calibration Factor	$\frac{1}{256}$	$\frac{1}{256}$	$\frac{1}{256}$	$\frac{1}{1285}$	$\frac{1}{1285}$	$\frac{1}{1289}$
Direct Reading	2679	2304	1194	2285	1803	1228
Reversed Reading	2622	2292	1623	2232	3358	891
Difference	57	12	429	53	1555	337
Scale Factor	4	4	4	1	1	1
Unit Load Reactions	0.891	-0.188	-6.710	0.041	-1.210	0.026
Reactions Due to Reversed Loading	-0.891	0.188	6.710	-0.041	1.210	-0.026
Units	kip-ft	kip-ft	kip-ft	kips	kips	kips

TABLE XA

CONSUMPTION OF REACTIONS DUE TO A UNIT LOAD AT
B PARALLEL TO BF IN Y DIRECTION FROM B TOWARD F

Component	M_{AX} / I	M_{AY} / I	R_{AX} / I	R_{AY} / I	R_{BX} / I
Fixed Support	250	525	1252	1252	1382
Cantilever Portion					
Direct Reactions					
Redundant	5696	1194	2282	1303	1338
Beavered					
Redundant	5696	1633	2282	3328	681
Difference	13	439	13	1252	132
Basis Fixed	4	4	1	1	1
Unit Load					
Reactions	0.881	-0.170	0.047	-1.510	0.050
Reactions Due to Beavered					
Fossil	-0.188	0.170	-0.047	1.510	-0.050
Unit	42-gin	Kip-ft	Kip	Kip	Kip

TABLE XVI

COMPUTATION OF REACTIONS DUE TO A VERTICAL UNIT LOAD ACTING DOWN AT E

Component	M_{Axy}	M_{Axz}	M_{Ayz}	R_{Ax}	R_{Ay}	R_{Az}
Calibration Factor	$\frac{1}{256}$	$\frac{1}{256}$	$\frac{1}{256}$	$\frac{1}{1285}$	$\frac{1}{1285}$	$\frac{1}{1289}$
Direct Reading	2326	1078	2923	530	2494	1118
Reversed Reading	2326	1078	3030	563	3249	1025
Difference	0	0	107	33	755	93
Scale Factor	4	4	4	1	1	1
Unit Load Reactions	0	0	-1.672	0.026	0.588	-0.072
Reactions Due to Reversed Loading	0	0	1.672	-0.026	-0.588	0.072
Units	kip-ft	kip-ft	kip-ft	kips	kips	kips

TABLE XVI

COMPARISON OF REACTIONS DUE TO A UNIFORM LOAD ACTING UNIT LOAD APART FROM BOTH AT B

Component	M_A^{UNIT}	M_A^{UNIT}	R_A^{UNIT}	R_A^{UNIT}	R_B^{UNIT}
	$\frac{1}{2}$	$\frac{1}{2}$	$\frac{1}{2}$	$\frac{1}{2}$	$\frac{1}{2}$
Continuous beam	5525	7078	5030	5494	7118
Propped cantilever	5525	7078	5030	5494	7118
Direct	5525	7078	5030	5494	7118
Reversed	5525	7078	5030	5494	7118
Bending

TABLE XVII

COMPUTATION OF REACTIONS DUE TO A UNIT LOAD AT F PARALLEL TO CD IN A DIRECTION FROM C TOWARD D

Component	M_{Axy}	M_{Axz}	M_{Ayz}	R_{Ax}	R_{Ay}	R_{Az}
Calibration Factor	$\frac{1}{256}$	$\frac{1}{256}$	$\frac{1}{256}$	$\frac{1}{1289}$	$\frac{1}{1289}$	$\frac{1}{1295}$
Direct Reading	2499	2385	638	2444	2041	804
Reversed Reading	2519	2355	1046	2348	2959	540
Difference	20	30	408	96	918	264
Scale Factor	4	4	4	1	1	1
Unit Load Reactions	-0.313	0.469	6.380	-0.075	0.713	-0.240
Reactions Due to Reversed Loading	0.313	-0.469	-6.380	0.075	-0.713	0.240
Units	kip-ft	kip-ft	kip-ft	kips	kips	kips

TABLE XVIII

F RATIOS TO CD IN A DISTINCTION FROM C FORMED B

Component	M_{xx}	M_{xy}	M_{yy}	$\frac{M_{xx}}{f}$	$\frac{M_{xy}}{f}$	$\frac{M_{yy}}{f}$	F_{xx}	F_{xy}	F_{yy}
Optimum motor	$\frac{S_{xx}}{f}$	$\frac{S_{xy}}{f}$							
Direct methods	2449	638	2021	2449	638	2021	804		
Reasoning	3285	1065	3455	3285	1065	3455	540		
Subjects	5734	1703	5476	5734	1703	5476	940		
Differences	98	40	98	98	40	98	244		
Basis factor	4	4	1	4	4	1	1		
Unit load									
Regression	-0.713	0.498	-0.018	0.373	-0.380	0.013	-0.340		
Residuals due to Regression	-0.498	-0.498	-0.498	-0.498	-0.498	-0.498	0.340		
Total	0.713	-0.498	0.018	0.373	-0.380	0.013	0.340		
Units	kip-ft	kip-ft	kip-ft	kips	kips	kips	kips		

TABLE XVIII

COMPUTATION OF REACTIONS DUE TO A UNIT LOAD AT F PARALLEL TO EF IN A DIRECTION FROM E TOWARD F

Component	M_{Axy}	M_{Axz}	M_{Ayz}	R_{Ax}	R_{Ay}	R_{Az}
Calibration Factor	$\frac{1}{256}$	$\frac{1}{256}$	$\frac{1}{256}$	$\frac{1}{1289}$	$\frac{1}{1289}$	$\frac{1}{1295}$
Direct Reading	2651	2578	1288	2564	1865	1339
Reversed Reading	2659	2586	1725	2506	3375	991
Difference	8	8	437	58	1510	348
Scale Factor	4	4	4	1	1	1
Unit Load Reactions	0.125	0.125	-6.340	0.045	-1.171	0.269
Reactions Due to Reversed Loading	-0.125	-0.125	6.340	-0.045	1.171	-0.269
Units	kip-ft	kip-ft	kip-ft	kips	kips	kips

TABLE XVIII

COMPUTATION OF REACTIONS DUE TO A UNIT LOAD AT
1 FEMOTED TO 5F IN A DIRECTION FROM 3 TOWARD 1

Component	M_{1F}^{3F}	M_{2F}^{3F}	M_{3F}^{3F}	R_{1F}^{3F}	R_{3F}^{3F}
	$\frac{qsa}{I}$	$\frac{qsa}{I}$	$\frac{qsa}{I}$	$\frac{qsa}{I}$	$\frac{qsa}{I}$
Carryover	2552	2552	1278	1278	1278
Reading	2552	2552	1278	1278	1278
Moment	5104	5104	2556	2556	2556
Reading	2552	2552	1278	1278	1278
Moment	7656	7656	3834	3834	3834
Distribute	8	8	4N	8B	8B
Reading	2552	2552	1278	1278	1278
Moment	10208	10208	5112	5112	5112
Scale Factor	4	4	4	4	4

TABLE XIX

COMPUTATION OF REACTIONS DUE TO A VERTICAL UNIT LOAD ACTING DOWN AT F

Component	M_{Axy}	M_{Axz}	M_{Ayz}	R_{Ax}	R_{Ay}	R_{Az}
Calibration Factor	$\frac{1}{256}$	$\frac{1}{256}$	$\frac{1}{256}$	$\frac{1}{1289}$	$\frac{1}{1289}$	$\frac{1}{1295}$
Direct Reading	2313	2078	1771	2649	3282	2683
Reversed Reading	2303	2078	1866	2649	3454	2663
Difference	10	0	95	0	171	20
Scale Factor	4	4	4	1	1	1
Unit Load Reactions	0.156	0	-1.484	0	-0.133	-0.016
Reactions Due to Reversed Loading	-0.156	0	1.484	0	0.133	0.016
Units	kip-ft	kip-ft	kip-ft	kips	kips	kips

TABLE XIV

COMPARISON OF REACTIONS DUE TO A VERTICAL DEAD LOAD ACTING DOWN AT 1

TABLE XX

DETERMINATION OF UNIT LOAD REACTIONS AT B, C, AND D BY OBSERVATION OF SYMMETRY CONDITIONS

Component	Load, as in Table XIV	Load, as in Table XV	Load, as in Table XVI	Load, as in Table XVII	Load, as in Table XIX	Units
M_{Bxy}	6.520	6.170	1.672	6.340	-1.484	kip-ft.
M_{Bxz}	0.188	0.188	0	-0.125	0	kip-ft.
M_{Byz}	0.891	-0.891	0	-0.125	-0.156	kip-ft.
R_{Bx}	0.257	0.262	-0.072	0.269	-0.016	kips
R_{By}	-1.210	-1.210	0.588	-1.171	-0.133	kips
R_{Bz}	-0.301	0.041	0.026	0.045	0	kips
M_{Cxy}	-0.313	0.125	-0.156	0.891	0	kip-ft.
M_{Cxz}	-0.469	-0.125	0	-0.188	0	kip-ft.
M_{Cyz}	6.380	-6.340	-1.484	-6.710	1.672	kip-ft.
R_{Cx}	-0.075	0.045	0	0.041	-0.026	kips
R_{Cy}	-0.713	1.171	-0.133	1.210	0.588	kips
R_{Cz}	-0.204	0.269	0.016	0.262	0.072	kips

TABLE XX

DISPLACEMENT OF UNIT LOAD REACTIONS AT B, C,
AND D BY OBSERVATION OF SYMMETRY CONDITIONS

Component	Table XIV	Table XV	Load, as in Table XVI	Load, as in Table XIX	Units
M_{DY}	6.520	6.170	1.670	6.340	kip-ft.
M_{BX}	0.188	0.188	0	0	kip-ft.
M_{BY}	0.851	-0.851	0	-0.152	kip-ft.
B_X	0.257	0.252	-0.072	0.259	kips
B_Y	-1.210	-1.210	0.588	-1.173	kips
M_{CX}	-0.313	0.125	-0.156	0.881	kip-ft.
M_{CY}	-0.459	-0.125	0	-0.188	kip-ft.
B_Z	6.360	-6.360	-1.660	-6.110	kips
M_{DX}	-0.075	0.065	0.011	-0.032	kips
M_{DY}	-0.204	0.369	0.092	0.072	kips

TABLE XX (CONTINUED)

Component	Load, as in Table XIV	Load, as in Table XV	Load, as in Table XVI	Load, as in Table XVII	Load, as in Table XIX	Units
M_{Dxy}	0.891	6.430	1.484	6.710	-1.672	kip-ft.
M_{Dxz}	0.188	0.125	0	0.188	0	kip-ft.
M_{Dyz}	6.520	-0.125	0.156	-0.891	0	kip-ft.
R_{Dx}	0.301	0.269	0.016	0.262	0.072	kips
R_{Dy}	1.210	1.171	-0.133	1.210	0.588	kips
R_{Dz}	-0.257	0.045	0	0.041	-0.026	kips

TABLE XX (CONTINUED)

Component	Table XIV	Table XV	Table XVII	Table XIX	Unity
Apply	0.891	0.430	1.464	6.710	Imp-ft.
Open	0.158	0.158	0	0.158	Kip-ft.
Apply	6.320	-0.132	0.756	-0.891	Kip-ft.
Apply	0.891	0.158	0.015	0.803	Kip
Apply	1.470	-0.132	-0.132	4.320	Kip
Open	0.158	0.158	0	0.158	Kip

TABLE XXI

DETERMINATION OF REACTIONS DUE TO COMBINED LOADS

Component	Load, as in Table XIV	Load, as in Table XV	Load, as in Table XVI	Load, as in Table XVII	Load, as in Table XIX	Total	Units
Load Factor	5	0.5	1	1	2		
M_{Axy}	4.455	0.446	0	0.125	0.312	5.338	kip-ft.
M_{Axz}	0.940	-0.094	0	0.125	0	0.971	kip-ft.
M_{Ayz}	32.600	-3.355	-1.672	-6.340	2.968	24.201	kip-ft.
R_{Ax}	1.505	0.021	0.026	0.045	0	1.597	kips
R_{Ay}	6.050	-0.605	0.588	-1.171	-0.266	4.596	kips
R_{Az}	- 1.285	0.131	-0.072	0.269	-0.032	-0.989	kips
M_{Bxy}	32.600	3.355	1.672	6.340	-2.968	40.999	kip-ft.
M_{Bxz}	0.940	0.094	0	-0.125	0	0.909	kip-ft.
M_{Byz}	4.455	-0.446	0	-0.125	-0.312	3.572	kip-ft.
R_{Bx}	1.285	0.131	-0.072	0.269	-0.032	1.581	kips

TABLE XXI

DETERMINATION OF REACTIONS DUE TO COMBINED LOADS

Component	Load at in Table XIV	Load, as in Table XV	Load, as in Table XVI	Load, as in Table XVII	Total	Units
Load Factor	5	0.5	1	2		
M_{AX}	4.458	-0.446	0	0.252	4.338	kip-ft.
M_{AY}	0.040	-0.004	0	0.152	0.571	kip-ft.
M_{BX}	22.500	-2.250	-1.610	2.030	24.720	kip-ft.
M_{BY}	6.020	-0.602	0.588	-1.172	4.934	kip-ft.
R_{AX}	1.205	0.051	0.056	0.045	1.357	kips
R_{AY}	- 1.285	0.128	-0.072	0.588	-0.589	kips
R_{BX}	32.000	3.200	1.672	0.340	37.212	kips
R_{BY}	0.240	0.024	0.024	0.152	0.440	kips

TABLE XXI (CONTINUED)

Component	Load, as in Table XIV	Load, as in Table XV	Load, as in Table XVI	Load, as in Table XVII	Load, as in Table XIX	Total	Units
R_{By}	-6.050	-0.605	0.588	-1.171	-0.266	-7.504	kips
R_{Bz}	-1.505	0.021	0.026	0.045	0	-1.413	kips
M_{Cxy}	-1.565	0.063	-0.156	0.891	0	-0.767	kip-ft.
M_{Cxz}	-2.345	-0.063	0	-0.188	0	-2.596	kip-ft.
M_{Cyz}	31.900	-3.170	-1.484	-6.710	3.344	23.880	kip-ft.
R_{Cx}	-0.375	0.023	0	6.041	-0.052	-0.363	kips
R_{Cy}	-3.565	0.586	-0.133	1.210	1.176	-0.726	kips
R_{Cz}	-1.020	0.135	0.016	0.262	0.144	-0.463	kips
M_{Dxy}	31.900	3.170	1.484	6.710	-3.344	39.920	kip-ft.
M_{Dxz}	-2.345	0.063	0	0.188	0	-2.094	kip-ft.
M_{Dyz}	-1.565	-0.063	0.156	-0.891	0	-2.363	kip-ft.

TABLE XII (CONTINUED)

Component	Load, as in Table XIV	Load, as in Table XV	Load, as in Table XVI	Load, as in Table XIX	Total	Units
B_{XY}	-0.020	-0.005	0.588	-0.256	-7.504	kips
B_{ZX}	-1.505	0.021	0.026	0.040	-1.443	kips
M_{CXY}	-1.585	0.063	0.851	0	-0.767	kip-ft.
M_{CZX}	-3.348	-0.003	-0.188	0	-2.539	kip-ft.
M_{BXY}	31.800	-3.170	-6.710	3.344	23.880	kip-ft.
M_{BZX}	80.375	0.029	6.041	-0.032	-0.363	kips
B_{CY}	-3.585	0.588	-0.133	1.210	-0.726	kips
B_{CX}	-1.020	0.135	0.016	0.262	-0.446	kips
M_{BXY}	31.800	3.170	1.484	6.710	-3.344	kip-ft.
M_{BZX}	-2.345	0.063	0	0.188	-2.094	kip-ft.
M_{CXY}	-1.565	-0.063	0.345	0.891	-0.393	kip-ft.

TABLE XXI (CONTINUED)

Component	Load, as in Table XIV	Load, as in Table XV	Load, as in Table XVI	Load, as in Table XVII	Load, as in Table XIX	Total	Units
R_{Dx}	1.020	0.135	0.016	0.262	0.144	1.577	kips
R_{Dy}	3.565	0.586	-0.133	1.210	1.176	6.404	kips
R_{Dz}	0.375	0.023	0	0.041	-0.052	0.387	kips

TABLE XXI (CONTINUED)

Component	Load, as in Table XIV	Load, as in Table XV	Load, as in Table XVI	Load, as in Table XIX	Total	Data
B_{gx}	1.020	0.135	0.252	0.144	1.551	kg_f
B_{gy}	3.505	0.505	-0.733	1.716	6.404	kg_f
B_{gz}	0.373	0.023	0.041	-0.052	0.387	kg_f

APPENDIX C

KODAPAK CHARACTERISTICS AND PROPERTIES

Method of Manufacture	Extruded
Specific Gravity	1.22
Permanence	
Weight Loss, 6 hrs. @ 100°C., %	.25-.35
Shrinkage in Air, %	
24 hrs. @ 160°F. (dry)	0-.15
3 months @ 80°F., (60% relative humidity)	.1-.3
Discoloration Under Sunlamp (16 hrs.)	none
Mechanical	
Tensile Strength (parallel to grain), 10^3 psi.	5 - 6
Ultimate Elongation, %	60-100
Modulus of Toughness, in-lbs/cu.in. x 10^3	9 - 12
Modulus of Elasticity in Tension, 10^5 psi.	2.0-2.5
Thermal	
Flamability - Burning Rate, in./min.	2 - 3
Coefficient of Thermal Expansion (0° to 100°F.), in/in per degree F x 10^{-5}	6.5-7.5